AD-A232 950

DTIC FILE COPY

REPORT DOCUMENTATION PAGE

Form Approved
OMB No. 0704-0188

(2)

Public reporting burden for this collection of information is estimated to average 1 hour per response, including the time for reviewing instructions, searching existing data sources, gathering and maintaining the data needed, and completing and reviewing the collection of information. Send comments regarding this burden estimate or any other aspect of this collection of information, including suggestions for reducing this burden, to Washington Headquarters Services, Directorate for Information Operations and Reports, 1215 Jefferson Davis Highway, Suite 1204, Arlington, VA 22202-4302, and to the Office of Management and Budget, Paperwork Reduction Project (0704-0188), Washington, DC 20503.

AGENCY USE ONLY (*Leave blank*)	2. REPORT DATE 1/28/91	3. REPORT TYPE AND DATES COVERED Final; 6/15/87 - 11/30/90

TITLE AND SUBTITLE

Doping and Diffusion in HgCdTe

5. FUNDING NUMBERS

DAAL 03-87-K-0061

AUTHOR(S)

C. G. Morgan-Pond

PERFORMING ORGANIZATION NAME(S) AND ADDRESS(ES)

Physics Department
Wayne State University
Detroit MI 48202

PERFORMING ORGANIZATION REPORT NUMBER

DTIC
MAR 1 5 1991
S G

SPONSORING/MONITORING AGENCY NAME(S) AND ADDRESS(ES)

U. S. Army Research Office
P. O. Box 12211
Research Triangle Park, NC 27709-2211

10. SPONSORING/MONITORING AGENCY REPORT NUMBER

ARO 24837.11-MS

11. SUPPLEMENTARY NOTES

The view, opinions and/or findings contained in this report are those of the author(s) and should not be construed as an official Department of the Army position, policy, or decision, unless so designated by other documentation.

12a. DISTRIBUTION/AVAILABILITY STATEMENT

Approved for public release; distribution unlimited.

12b. DISTRIBUTION CODE

13. ABSTRACT (*Maximum 200 words*)

The structural properties and electrical activity of impurity (indium, arsenic, antimony) and self-interstitials (mercury, cadmium, tellurium) in CdTe and HgCdTe alloys have been studied by theoretical and computer calculations. The problems addressed included:

- the source of the midgap tunneling levels in Hg-rich HgCdTe,
- the cause of electrical inactivity in In-doped CdTe grown by non-photoassisted molecular beam epitaxy (MBE),
- identification of paths for impurity and self-diffusion,
- the effects of lattice distortion on defect properties and interactions.

14. SUBJECT TERMS

Point Defects, Interstitials, Diffusion, Semiconductors (Materials), Mercury Tellurides, Cadmium Tellurides

15. NUMBER OF PAGES

71

16. PRICE CODE

17. SECURITY CLASSIFICATION OF REPORT	18. SECURITY CLASSIFICATION OF THIS PAGE	19. SECURITY CLASSIFICATION OF ABSTRACT	20. LIMITATION OF ABSTRACT
UNCLASSIFIED	UNCLASSIFIED	UNCLASSIFIED	UL

NSN 7540-01-280-5500

Standard Form 298 (Rev. 2-89)
Prescribed by ANSI Std. Z39-18
298-102

DOPING AND DIFFUSION IN HgCdTe

FINAL REPORT

C. G. Morgan-Pond

January 28, 1991

U. S. ARMY RESEARCH OFFICE

CONTRACT NUMBER DAAL 03-87-K-0061

WAYNE STATE UNIVERSITY

APPROVED FOR PUBLIC RELEASE;
DISTRIBUTION UNLIMITED

91 2 19 048

THE VIEWS, OPINIONS, AND/OR FINDINGS CONTAINED IN THIS REPORT ARE THOSE OF THE AUTHOR(S) AND SHOULD NOT BE CONSTRUED AS AN OFFICIAL DEPARTMENT OF THE ARMY POSITION, POLICY, OR DECISION, UNLESS SO DESIGNATED BY OTHER DOCUMENTATION.

TABLE OF CONTENTS

LIST OF APPENDIXES ii

A. STATEMENT OF THE PROBLEM STUDIED 1

B. SUMMARY OF THE MOST IMPORTANT RESULTS 2

- 1. Characterization of Interstitial Defect States 2
  - a. Electronic Deep Levels and Electrical Activity 4
  - b. Total Energies and Diffusion Barriers 7
- 2. Effects of Lattice Distortion on Defect Properties and Interactions 7

C. LIST OF ALL PUBLICATIONS AND TECHNICAL REPORTS 9

D. LIST OF ALL PARTICIPATING SCIENTIFIC PERSONNEL AND ADVANCED DEGREES EARNED WHILE EMPLOYED ON THE PROJECT 11

REPORT OF INVENTIONS 11

BIBLIOGRAPHY 12

Accesion For

NTIS CRA&I ☑
DTIC TAB ☐
Unannounced ☐
Justification ....

By ....
Distribution /

Availability Codes

Dist	Avail and / or Special
A-1	

QUALITY INSPECTED 3

LIST OF APPENDIXES

APPENDIX A: Deep Interstitial Levels in $Hg_{1-x}Cd_xTe$

APPENDIX B: Interstitial Total Energies and Diffusion Barriers in $Hg_{1-x}Cd_xTe$

APPENDIX C: Point Defects with Lattice Distortion in CdTe and HgCdTe

APPENDIX D: Formation Mechanisms of Localized Interstitial States in Tetrahedrally Bonded Semiconductors

APPENDIX E: Present Status and Future of Theoretical Work on Point Defects and Diffusion in Semiconductors

A. STATEMENT OF THE PROBLEM STUDIED

The work carried out under this contract consisted of theoretical and computer calculations of the electrical and structural properties of various point defects which are likely to be electrically active in CdTe and HgCdTe alloys. These electrically active defects included both impurity (indium, arsenic, antimony) and self-interstitials (mercury, cadmium, tellurium). The major questions addressed in this work were:

1) How do these defects diffuse, and what determines their final distribution in the lattice?

2) How does the electrical activity of these defects change as a function of their position in the lattice?

Techniques used to address these questions included a tight-binding small-basis, or "local matrix", approach for estimating point defect total energies, electronic levels, and the character of the localized states, developed for covalently bonded materials with considerable ionic and metallic character, such as HgCdTe,[1-6] and a more quantitatively accurate tight-binding supercell approach, which was used to investigate the effects of lattice distortion.[7-8] The local matrix method was primarily developed under a previously awarded ARO contract (DAAG 29-85-0119), and it is more fully discussed in the reports for this contract, although the final two papers giving an extensive description of this method[5-6] were prepared under the present contract. The bulk of the work supported by the present contract consisted of using the methods developed under both contracts to investigate problems of practical interest to those making devices using CdTe and HgCdTe alloys, such as the electrical inactivity which is often observed for a large fraction of the indium added to CdTe by non-laser-assisted molecular beam epitaxy (MBE).[9]

This contract was funded in part by the Night Vision and Electro-Optics Center (NVEOC), which has a major interest in developing and improving devices based on CdTe and HgCdTe alloys. The physical insight into dopant and native defect behavior derived from the theoretical results described in the body of this report was made available to researchers working with $Hg_{1-x}Cd_xTe$ and growing InSb/CdTe heterojunctions at the NVEOC through a series of formal and informal talks.

SIMS experiments on diffusion in CdTe, HgTe, and HgCdTe alloys at the NVEOC, designed to provide data for theoretical interpretation and to test theoretical conclusions, were planned to proceed in parallel with the theoretical work funded under this contract. Due to equipment problems and funding constraints at NVEOC, these experiments have not yet progressed beyond the calibration and testing stage, and comparison of the theoretical results obtained with experimental results for diffusion in CdTe, HgTe, and HgCdTe was limited to a review of the existing experimental (and theoretical) literature.[10]

B. SUMMARY OF THE MOST IMPORTANT RESULTS

1. Characterization of Interstitial Defect States

Previous calculations[11-13] demonstrated that both CdTe and Hg-rich HgCdTe tend to have high total concentrations of point defects during growth and annealing, whether or not electrically active impurities have been added. Substantial equilibrium concentrations of both vacancies and interstitials were predicted under various growth and annealing conditions.

It was also suggested[11,13] that the macroscopic quality of the final crystal depends on kinetic processes which may be strongly affected by lattice strains associated with impurities such as zinc. (These strains may pin the point defects generated at growth, inhibiting their condensation into larger extended defects, and perhaps explaining[11,13] the dramatic decrease in dislocation densities seen in $Cd_{0.96}Zn_{0.04}Te$, as compared with CdTe.[14]) Defect diffusion can control the electrical uniformity and stability over time of doped materials, heterojunctions, and superlattices, as well as the formation of macroscopic defects such as dislocations. While vacancies and substitutional and antisite defects may be more numerous, interstitial defects tend to move easily within the crystal and often make the most significant contribution to diffusion.

Occupation of various defect sites, and the resulting equilibrium and kinetic properties, may be strongly dependent on the technological processes used to prepare the alloy for device applications. For example, in nonequilibrium situations such as occur in material processed at low temperatures, quenched after high-temperature growth or annealing, or damaged by radiation,[15] substitutional impurities may be preferentially displaced to interstitial positions. If it occurs, this displacement will affect both the diffusion and electrical behavior of substitutional dopants such as indium.

The first part of the work for this project included an investigation of the total energies and deep electronic defect levels associated with various impurity and self-interstitials at different sites in the lattice (as well as a few substitutional defects), and the implications of these results for diffusion and electrical behavior, including dopant self-compensation. The major conclusions are summarized in Sections a and b below, and discussed in greater detail in the papers included as Appendixes A and B, and the other cited papers included in the list of publications.

In addition to accurately showing trends in the electronic defect levels and total energies, the local matrix method used in these calculations allows us to form a good qualitative picture of the charge distribution associated with the localized defect states. In the absence of reproducible experimental characterizations of the localized electronic states of these point defects, the calculated wave functions may be used to estimate carrier capture cross sections, and to investigate the changes in bonding at the defect site which may occur as a result of charge carrier capture. The local matrix method also gives a particularly clear physical understanding of the role of the local environment in determining the character of the localized defect states.[6]

As an example of this characterization, Figure 4 in Appendix D shows the formation process of the localized defect states from the interstitial atomic orbitals and the sp-bonding hybrids of the neighboring anions and cations for the mercury interstitial at the preferred tetrahedral position in CdTe. At each stage, the fraction of the total charge distribution on the interstitial, the nearest neighbor shell, and the shell of atoms bonded to the nearest neighbors is given for each localized level. The wave function for the A_1 tetrahedral interstitial level in the gap region is strongly concentrated on the mercury interstitial, in contrast to the wave function for the A_1 tetrahedral interstitial level of the phosphorus interstitial (with phosphorus nearest neighbors) in GaP, shown in Figure 1. This is explained as a result of the different ordering of the parent levels on the isolated atoms: both the s and p orbital energies for the mercury interstitial lie above the energy of the sp-bonding hybrids on the nearest-neighbor tellurium atoms, while the s orbital energy for the phosphorus interstitial lies below the energy of the sp-bonding hybrids on the nearest-neighbor phosphorus atoms.

a. Electronic Deep Levels and Electrical Activity

In order to test the reliability of the local matrix method for describing the localized deep and hyperdeep level structure, the results of local matrix calculations were compared with self-consistent Green's function and experimental results for various interstitials in Si and GaP,[5] and for substitutional defects, including vacancies, in Si, GaP, GaAs, and CdTe.[2] The results of these calculations were in substantial agreement with available experimental data for cation vacancies,[16] substitutional gallium and indium on cation sites,[17] and bromine on the anion site[17] in CdTe, as well as for the various defects considered in Si, GaP, and GaAs. There is a discrepancy for oxygen on the anion site in CdTe, since a level in the gap has been attributed to this defect,[18] while the local matrix calculation gives an A_1 level for this defect higher up, at 2.2 eV above the valence band edge, in the absence of lattice distortion. However, this discrepancy may be due to the existence of substantial lattice distortion, since oxygen is a small impurity, and tends to be associated with lattice distortion in other systems.

The original characterization of the localized defect states of indium and self-interstitials (Hg, Cd, Te) at tetrahedral and hexagonal positions in $Hg_{1-x}Cd_xTe$ is given in the paper attached as Appendix A.[1] The calculated energy trends and conclusions were unchanged by a subsequent minor modification of the parameters and the inclusion of a self-consistent treatment of the charge distribution.[5,6] Two major conclusions, discussed more fully in Appendix A, emerged from this work:

(i) A level of A_1 symmetry due to the mercury interstitial at the tetrahedral site between tellurium nearest neighbors (which was assumed to be the preferred tetrahedral site for mercury interstitials) was identified as a possible candidate for providing the midgap tunneling levels in Hg-rich HgCdTe.

(ii) It was shown that self-compensation by indium interstitials in the preferred tetrahedral site (assumed to be between tellurium nearest neighbors) cannot account for the electrical inactivity often observed for a large fraction of the indium added to CdTe by non-photoassisted MBE.[9]

Equilibrium defect densities were calculated for indium-doped CdTe at temperatures and pressures similar to those which occur during MBE growth,[19] using methods previously developed.[11,13] It was found that the addition of indium promotes the creation of cation vacancies. At low temperatures and high doping levels, a substantial fraction of the indium is bound in neutral complexes consisting of a single cation vacancy and two substitutional indium atoms, while nearly equal concentrations of positively charged substitutional indium and negatively charged complexes of a cation vacancy with a single substitutional indium compensate each other, leading to net charge carrier concentrations much lower than the total indium concentration.[19]

These results indicate that formation of indium-cation vacancy complexes can fully account for the observed electrical inactivity, if the material is close to equilibrium during growth. It was suggested that the high photon flux occurring during photoassisted MBE could excite a large number of free carriers at the growing surface, screening the Coulomb attraction between charged defects and inhibiting the formation of complexes.[19] X-ray rocking studies of the macroscopic crystal quality of samples grown by photoassisted and non-photoassisted MBE were suggested, to help determine whether the defects are able to approach equilibrium sufficiently so that indium-cation vacancy complex formation causes self-compensation, or whether the inactive indium is bound in extended (non-equilibrium) defects in the non-photoassisted samples. In the latter case, it was suggested that laser illumination of the substrate or the impinging atoms could provide enough energy to bring the system closer to equilibrium, and reduce concentrations of these non-equilibrium defects.[19]

b. Total Energies and Diffusion Barriers

The local matrix results for the total energies of interstitial defects in various positions in $Hg_{1-x}Cd_xTe$ are presented in the paper attached as Appendix B.[3] The major conclusions of this work, described in more detail in Appendix B, are summarized below:

(i) The preferred tetrahedral interstitial site for mercury, cadmium, and indium in $Hg_{1-x}Cd_xTe$ is between tellurium nearest neighbors. These results support the earlier assumptions we made[1] in identifying the mercury interstitial at this site as a likely candidate for providing midgap tunneling levels in Hg-rich HgCdTe, and arguing that self-compensation arising from indium interstitials is unlikely.

(ii) The preferred tetrahedral interstitial site for tellurium in $Hg_{1-x}Cd_xTe$ is between cation nearest neighbors.

(iii) Charge carrier capture lowers diffusion barriers for simple interstitial diffusion down the open channels in the lattice for all the interstitials considered.

(iv) Diffusion down these open channels may be important for mercury interstitials, but it appears to be less favorable for indium, and very unfavorable for cadmium, which must diffuse by some more complicated mechanism, probably involving exchange with atoms on the lattice sites. (These conclusions were in agreement with simultaneously reported experimental results.[20])

2. Effects of Lattice Distortion on Defect Properties and Interactions

Self-consistent tight-binding supercell calculations were carried out to investigate the lattice relaxation associated with vacancies and various impurity (indium, arsenic, antimony) and self-interstitial (mercury, cadmium, tellurium) defects in $Hg_{1-x}Cd_xTe$.[7,8] The results of this work are summarized in the paper attached as Appendix C.[8] The major conclusions drawn from this investigation, discussed in more detail in Appendix C, are listed below:

(i) The strain-mediated attraction found between tellurium interstitials and cation vacancies may promote the creation of antisite defects.

(ii) The large strain found for tellurium interstitials may help explain the tendency for excess tellurium to condense into tellurium inclusions.

(iii) The unfavorability of simple interstitial diffusion of cadmium down the open channels in the lattice which was predicted theoretically[3] and verified experimentally[20] is seen to be a consequence of the large strain energy for cadmium interstitials in the hexagonal and alternate tetrahedral sites.

(iv) The localized A_1 electronic state of the tetrahedral mercury interstitial identified above[1] becomes slightly more localized on the interstitial as a result of relaxation of the surrounding lattice, but it remains a candidate for providing midgap tunneling levels in Hg-rich HgCdTe.

Further work on improving the accuracy of these tight-binding supercell total energy calculations for a wide range of defects is still in progress. As a part of this work, a preliminary investigation of the role of the d states in determining the behavior of defects in CdTe and related alloys has begun.[21]

C. LIST OF ALL PUBLICATIONS AND TECHNICAL REPORTS

"Deep Interstitial Levels in $Hg_{1-x}Cd_xTe$", S. Goettig and C. G. Morgan-Pond, Extended Abstracts of the 1987 MCT Workshop, New Orleans, LA, October 6-8, 1987, O/DI-27.

"Interstitial Total Energies and Diffusion Barriers in $Hg_{1-x}Cd_xTe$", C. G. Morgan-Pond, S. Goettig, and J. T. Schick, Extended Abstracts of the 1988 MCT Workshop, Orlando, FL, October 11-13, 1988, IV-31.

"Deep Interstitial Levels in $Hg_{1-x}Cd_xTe$", S. Goettig and C. G. Morgan-Pond, J. Vac. Sci. Technol. A6, 2670 (1988).

"Localized States in Tetrahedrally Bonded Semiconductors", S. Goettig and C. G. Morgan-Pond, Materials Science Forum 38-41, 317 (1989).

"Interstitial Total Energies and Diffusion Barriers in $Hg_{1-x}Cd_xTe$", C. G. Morgan-Pond, J. T. Schick, and S. Goettig, J. Vac. Sci. Technol. A 7, 354 (1989).

"Formation Mechanisms of Interstitial Defect States", S. Goettig and C. G. Morgan-Pond, Proceedings of the XVIII International School on the Physics of Semiconducting Compounds, Jaszowiec, Poland, April 24-28, 1989.

"Point Defects with Lattice Distortion in CdTe and HgCdTe", J. T. Schick and C. G. Morgan-Pond, Extended Abstracts of the 1989 MCT Workshop, San Diego, CA, October 3-5, 1989, II-7.

"Structural Energies of Defects in CdTe and HgCdTe", J. T. Schick and C. G. Morgan-Pond, Semiconductor Science and Technology 5, S81 (1990).

"Point Defects with Lattice Distortion in CdTe and HgCdTe", J. T. Schick and C. G. Morgan-Pond, J. Vac. Sci. Technol. A8, 1108 (1990).

"Localized Interstitial States in Tetrahedrally Bonded Semiconductors - The Local Matrix Approach", S. Goettig and C. G. Morgan-Pond, Phys. Rev. B 42, 11730 (1990).

"Formation Mechanisms of Localized Interstitial States in Tetrahedrally Bonded Semiconductors", S. Goettig and C. G. Morgan-Pond, Phys. Rev. B 42, 11743 (1990).

"Present Status and Future of Theoretical Work on Point Defects and Diffusion in Semiconductors", C. G. Morgan-Pond, J. Electronic Materials, 1991, in press.

"Interstitial Bonding in CdTe: Role of the d States", J. T. Schick and C. G. Morgan-Pond, in preparation.

D. LIST OF ALL PARTICIPATING SCIENTIFIC PERSONNEL AND ADVANCED DEGREES EARNED WHILE EMPLOYED ON THE PROJECT

Professor C. G. Morgan-Pond, Principal Investigator

Dr. S. Goettig, Research Associate

Dr. J. T. Schick, Research Associate

REPORT OF INVENTIONS

Local Matrix Method:

A new theoretical approach for characterizing the localized defect states due to microscopic structural defects was developed, tested, and used to study defects in $Hg_{1-x}Cd_xTe$ under the present contract (DAAL 03-87-K-0061) and a previously awarded ARO contract (DAAG 29-85-K-0119). This method and its applications are described briefly in the final report for DAAG 29-85-K-0119, in the papers attached to this report as Appendixes A, B, and D, and in the other publications cited as references in this report. An extensive presentation of the method is given in Goettig and Morgan-Pond, Phy. Rev. B 42, 11730 (1990).

BIBLIOGRAPHY

[1] S. Goettig and C. G. Morgan-Pond, J. Vac. Sci. Technol. A6, 2670 (1988), included as Appendix A.

[2] S. Goettig and C. G. Morgan-Pond, Materials Science Forum 38-41, 317 (1989).

[3] C. G. Morgan-Pond, J. T. Schick, and S. Goettig, J. Vac. Sci. Technol. A7, 354 (1989), included as Appendix B.

[4] S. Goettig and C. G. Morgan-Pond, Proceedings of the XVIII International School on the Physics of Semiconducting Compounds, Jaszowiec, Poland, April 24-28, 1989.

[5] S. Goettig and C. G. Morgan-Pond, Phys. Rev. B 42, 11730 (1990).

[6] S. Goettig and C. G. Morgan-Pond, Phys. Rev. B 42, 11743 (1990), included as Appendix D.

[7] J. T. Schick and C. G. Morgan-Pond, Semiconductor Science and Technology 5, S81 (1990).

[8] J. T. Schick and C. G. Morgan-Pond, J. Vac. Sci. Technol. A8, 1108 (1990), included as Appendix C.

[9] R. N. Bicknell, N. C. Giles, and J. F. Schetzina, Appl. Phys. Lett. 49, 1095 (1986).

[10] C. G. Morgan-Pond, J. Electronic Materials, 1991, in press, included as Appendix E.

[11] C. G. Morgan-Pond and R. Raghavan, Phys. Rev. B31, 6616 (1985).

[12] C. G. Morgan-Pond, Proceedings of the ARO Infrared Materials Review, Raleigh, NC, February 11-12, 1986.

[13] C. G. Morgan-Pond and R. Raghavan, Materials Science Forum 10-12, 79 (1986).

[14] S. L. Bell and S. Sen, J. Vac. Sci. Technol. A3, 112 (1985).

[15] G. D. Watkins, Radiation Damage in Semiconductors, 97 (Dunod,1967).

[16] M. K. Lorenz and B. Segall, Phys. Lett. 7, 18 (1963), and F. Yamada, J. Phys. Soc. Japan 15, 1940 (1960).

[17] G. W. Iseler, J. A. Kafalas, A. J. Strauss, H. F. MacMillan, and R. H. Bube, Sol. St. Comm. 10, 619 (1972).

[18] N. V. Agrinskaya et al., Sov. Phys.-Semicond. 8, 202 (1974).

[19] C. G. Morgan-Pond, talk given on August 19, 1987 at NVEOC, unpublished.

[20] M.-F. Sung Tang and D. A. Stevenson, J. Vac. Sci. Technol. A 7, 544 (1989).

[21] J. T. Schick and C. G. Morgan-Pond, in preparation.

Deep interstitial levels in $Hg_{1-x}Cd_xTe$

S. Goettig[a] and C. G. Morgan-Pond
Department of Physics and Astronomy, Wayne State University, Detroit, Michigan 48202

(Received 3 November 1987; accepted 29 February 1988)

The deep levels of indium and self-interstitials (Hg,Cd,Te) in tetrahedral and hexagonal positions in $Hg_{1-x}Cd_xTe$ are characterized and energy trends are calculated within the defect-molecule approach. We have extended this method to include metallic and polar, as well as covalent, coupling. Possibilities for self-compensation due to interstitials in In-doped $He_{1-x}Cd_xTe$, and a possible candidate for the midgap tunneling centers in $Hg_{0.8}Cd_{0.2}Te$ are discussed.

I. INTRODUCTION

The identification of deep levels of various defects in $Hg_{1-x}Cd_xTe$ is an important step towards the understanding of the defect-induced behavior of these materials. While most of the unambiguously identified levels have been attributed to substitutional impurities,[1] knowledge about interstitial defects in HgCdTe is still rather fragmentary.

In this paper we develop a defect-molecule theory of deep localized states of neutral interstitial defects in $Hg_{1-x}Cd_xTe$. The linear combination of atomic orbitals (LCAO) defect-molecule method allows us to calculate the energies of the deep levels, their symmetries and occupancies, as well as the corresponding electronic charge densities. We extend the method,[5] recently applied to self-interstitials in Si,[6] to account for the metallic coupling (promotion energy) and the polar coupling, both of which are important in HgCdTe. This simple model allows us to form a qualitative picture of the localized interstitial levels, and to investigate energy trends for the deep levels. Ongoing work[16] has confirmed the insensitivity of the trends noted here to some of the approximations made. However, the calculated energy levels cannot be viewed as quantitatively reliable.

We consider a molecule (cluster) composed of the interstitial, its nearest neighbors, and all atoms bonded to the nearest neighbors. The cluster is separated from the bulk by systematically neglecting the promotion energy on all atoms bonded to the nearest neighbors of the interstitial, with no additional boundary condition imposed. Both tetrahedral and hexagonal positions of the interstitial are considered. The position of the valence band is calculated using the full sp^3 tight-binding scheme with the same parameters as are used in the defect level calculations.

In applying the formalism to HgCdTe, we have concentrated on indium and self-interstitials. Self-interstitials are of general interest as potentially ever-present elementary defects. It has also been suggested[2] that they might provide deep levels for the midgap tunneling observed in $Hg_{0.8}Cd_{0.2}Te$. The identification of such levels may have important practical applications.

The doping of $Hg_{1-x}Cd_xTe$ with indium has attracted much experimental attention, but is still not fully understood. When introduced in small concentrations at high temperature, indium acts primarily as a substitutional dopant with shallow donor levels. However, when indium is added to CdTe films during low-temperature [molecular-beam epitaxy (MBE)] growth, a large fraction of the indium is observed to be electrically inactive (except when added by photoassisted MBE[3]). It is known that substitutional impurities may be preferentially displaced to interstitial sites in material with high (nonequilibrium) densities of native defects resulting from radiation damage[4] or low-temperature growth. Thus, the electrical inactivity of indium when added to CdTe during low-temperature growth may be attributed to preferential displacement of In atoms from substitutional to interstitial sites, resulting in formation of interstitial deep acceptor levels which lead to self-compensation. We discuss this explanation based on the indium interstitial deep levels calculated within the present model.

II. THEORY

A. Defect-molecule model

Let us consider a tetrahedrally bonded crystal composed of N atoms of P different kinds ($a = 1,2,...,P$) and a neutral interstitial defect ($a = d$). We assume that both host and interstitial atoms have only s and p valence electrons, i.e., all d shells are closed and do not take part in the bonding. As a basis for the LCAO expansion, we can use one s-like ($\phi_s^{(a)}$) and three p-like ($\phi_x^{(a)},\phi_y^{(a)},\phi_z^{(a)}$) quasiatomic orbitals centered on each host and defect site. Equivalently, we may use sp^3 tetrahedrally directed hybrids $\varphi_{i,j}$, where $\phi_{i,j}$ denotes a hybrid centered on the ith site with the positive lobe pointing towards the jth nearest-neighbor site. Thus, the one-electron wave function of the system can be written in the convenient LCAO form:

$$\Psi(\mathbf{r}) = \sum_{i=1}^{N} \sum_{j(i)=1}^{4} \alpha_{i,j}\varphi_{i,j}(\mathbf{r}) + \sum_{s,x,y,z} \alpha_n \phi_n^{(d)}(\mathbf{r}) , \qquad (1)$$

with the first term referring to the host and the second to the defect. The origin of the reference frame was chosen at the interstitial site. The first index in $\varphi_{i,j}$ is multiple and describes both the position of the site $\mathbf{r}_i$ and the kind of atom occupying this site. The summation over j in Eq. (1) is over the four nearest-neighbor sites of the ith site. We use the Schrödinger equation $H\Psi = E\Psi$, where H is the total one-electron Hamiltonian consisting of the kinetic part and the potential part $V(\mathbf{r})$, due to interaction with the atomic cores and the (self-consistent) field due to all other electrons. This gives the matrix equation

$$\sum_{i=0}^{N} \sum_{j(i)=1}^{4} \alpha_{i,j}\{\langle\varphi_{i',j'}|H|\varphi_{i,j}\rangle - E\delta_{ii'}\delta_{jj'}\} = 0, \qquad (2)$$

where the compact notation $\varphi_{0,n} \equiv \phi_n^{(d)}$, $\alpha_{0,n} \equiv \alpha_n$ has been introduced. All orbital overlaps were neglected in Eq. (2).

Considering on-site matrix elements in Eq. (2), for the host sites ($i \neq 0$) we have

$$\langle \varphi_{i,j} | H | \varphi_{i,j'} \rangle = \begin{cases} (1/4)(E_s^{(a)} + 3E_p^{(a)}) = E_a & \text{for } j = j' \\ (1/4)(E_p^{(a)} - E_s^{(a)}) = \Delta_a & \text{for } j \neq j' \end{cases}, \tag{3}$$

where

$$E_s^{(a)} = \langle \phi_s^{(a)} | H | \phi_s^{(a)} \rangle, \tag{4a}$$

$$E_p^{(a)} = \langle \phi_x^{(a)} | H | \phi_x^{(a)} \rangle. \tag{4b}$$

Polar coupling (in nonhomopolar crystals) is due to different values of E_a for anions and cations, while metallic coupling is due to nonzero promotion energy $4\Delta_a$. We are assuming here that the on-site matrix elements are determined by the local (on-site) behavior of the potential $V(\mathbf{r})$, neglecting the influence of the interstitial on their values. (E_a and Δ_a depend on the kind of atom but not its position relative to the interstitial.) The nonvanishing on-site matrix elements for the defect site are given by Eq. (4) with $a = d$.

The off-site matrix elements in Eq. (2) are considered within the nearest-neighbor and two-center[7] approximations, i.e., they are described by four parameters: $V_{ss\sigma}$, $V_{sp\sigma}$, $V_{pp\sigma}$, and $V_{pp\pi}$. Considering matrix elements between host hybrids, we make the further simplification of including only the interaction between hybrids pointing towards each other (covalent coupling)

$$\langle \varphi_{i,j} | H | \varphi_{j,i} \rangle = \beta, \tag{5}$$

neglecting here other, weaker,[5] interactions between nearest-neighbor hybrids. Here $\beta = (V_{ss\sigma} - 2\sqrt{3}V_{sp\sigma} - 3V_{pp\sigma})/4$. The interaction between the defect and its nearest neighbors will be considered in the next subsections.

The separation of the defect molecule from the crystal is an approximate procedure in which certain matrix elements in Eq. (2) are neglected. We have chosen the molecule to consist of the interstititial, its first nearest neighbors (1*nn*), and all atoms bonded to first nearest neighbors (2*nn*), in both tetrahedral and hexagonal positions (Fig. 1). This is the smallest reasonable cluster which can be chosen without breaking any covalent bonds (the strongest coupling in the crystal). The separation of this molecule from the crystal consists of neglecting Δ_a (the promotion energy) on all 2*nn* atoms.

The choice of the cluster is important, and adding a few more shells to a small cluster does not always give better results.[8] In choosing the cluster, we were led by two criteria. First, all bonds which are most affected by the presence of the interstitial (i.e., bonding involving 1*nn* atoms, which are overcoordinated due to the presence of the interstitial) were systematically included. Second, inclusion of bulklike bonds between tetrahedrally coordinated host atoms was avoided. These bonds are included in calculations for large clusters, consisting of 2000 or more atoms. However, inclusion of less than a macroscopically large number of bulklike bonds in small-cluster calculations causes the mixing in of poorly described extended states which are not true bulk states. Although this correctly represents the tendency of the charge distribution to spread out beyond the 2*nn* atoms, the calculated energy levels often turn out empirically[9] to be closer to the true macroscopic limit for clusters which include only bonds involving under- or overcoordinated atoms than for clusters which include a moderate number of bonds between properly coordinated atoms as well. Although the actual charge density associated with a defect level extends beyond the boundaries of the small cluster we have chosen, the *relative* charge densities on the different ions closest to the defect have been shown to be relatively unaffected in calculations of this kind when the size of the cluster is extended.[16]

B. Tetrahedral interstitial

In this case, the molecule consists of 15 atoms and involves 36 basis states. Four states are located on the interstitial. There are four 1*nn* atoms, each with a total of eight states involved in its four bonds to 2*nn* atoms, thus accounting for the 32 other basis states. Since six of the 2*nn* atoms are bonded to two 1*nn* atoms, there are ten 2*nn* atoms in all [see Fig. 1(a)]. We note that because Δ_a on 2*nn* atoms was neglected, the molecule can be seen as consisting of the interstitial and four side clusters (each containing five host atoms) coupled to each other only through the interstitial.

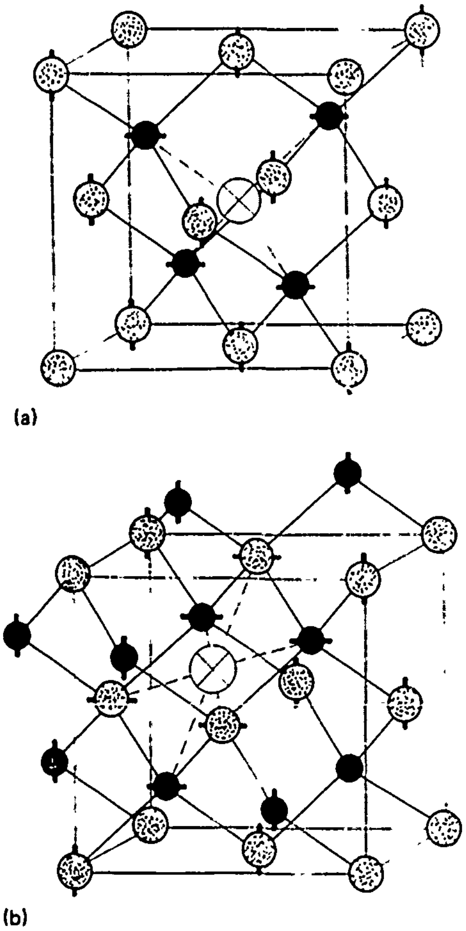

FIG. 1. Defect molecules used for (a) tetrahedral and (b) hexagonal interstitials in the zinc-blende lattice. The defect is indicated by ⊗, the 1*nn* atoms are marked with a horizontal bar, and 2*nn* atoms are marked with a vertical bar. Cations and anions are indicated by ○ and ● (or vice versa)

Since the interstitial is tetrahedrally coordinated, it is convenient to choose the basis on the defect to be four tetrahedrally directed hybrids. Then we can assume that the hybrids on a given $1nn$ atom couple only to the interstitial hybrid which points toward this atom. The couplings with the other three interstitial hybrids are roughly an order of magnitude smaller, and shall not be considered here. The addition of these couplings changes the energies of the deep levels within 1 eV of the gap by <0.2 eV.[16]

The 36×36 matrix for the tetrahedral interstitial in the zinc-blende crystal ($P=2$) was diagonalized analytically Omitting the details of the calculation, we only mention that the diagonalization relies on representing the Hamiltonian matrix in Eq. (2) in the basis consisting of the eigenfunctions of the five-atom side clusters, and then using the Löwdin[10] transformation. The deep-level energies E are then given exactly as the solutions of the following fifth-order equations:

$$E-\epsilon=\left\{\frac{|c_{s+}|^2\beta_s^2}{E-E_{s+}}+\frac{|c_{s-}|^2\beta_s^2}{E-E_{s-}}\right.$$

$$\left.+3\,\frac{|c_{p+}|^2\beta_p^2}{E-E_{p+}}+\frac{|c_{p-}|^2\beta_p^2}{E-E_{p-}}\right\}, \qquad (6)$$

with $\epsilon = E_s^{(d)}$ for the nondegenerate state of A_1 symmetry, and $\epsilon = E_p^{(d)}$ for the threefold degenerate state of T_2 symmetry. Here,

$$E_{s\pm} = (1/2)\{E_1 - 3\Delta_1 + E_2$$

$$\pm\sqrt{(E_1-3\Delta_1-E_2)^2+4\beta^2}\}, \qquad (7)$$

$$E_{p\pm} = (1/2)\{E_1 + \Delta_1 + E_2$$

$$\pm\sqrt{(E_1+\Delta_1-E_2)^2+4\beta^2}\}, \qquad (8)$$

$$c_{s\pm} = (1/2)\{1+\beta^2/(E_{s\pm}-E_2)^2\}^{-1/2}, \qquad (9)$$

$$c_{p\pm} = (1/2)\{1+\beta^2/(E_{p\pm}-E_2)^2\}^{-1/2}, \qquad (10)$$

are the eigenvalues and the normalization factors for the eigenfunctions of the five-atom cluster. We note that all $1nn$ atoms are of the same kind (either cations or anions), and all $2nn$ atoms are of the opposite kind. In Eqs. (7) and (8), E_1 and Δ_1 refer to $1nn$ atoms, while E_2 refers to $2nn$ atoms. The parameters $\beta_s = V_{ss\sigma} - 3V_{sp\sigma}$ and $\beta_p = -V_{sp\sigma} - V_{pp\sigma}$ describe the coupling of the s and p orbitals on the $1nn$ atom. We note that in the absence of the interstitial ($\epsilon\to\infty$), the energy levels of the defect molecule are given by Eqs. (7) and (8).

The formulas obtained for the corresponding wave functions are rather complicated and will not be presented here.

C. Hexagonal interstitial

In this case the molecule consists of 19 atoms and involves 40 basis states. Again, four of these states are located on the interstitial. Each of the six $1nn$ atoms is bonded to two $2nn$ atoms and two other $1nn$ atoms, so that the six $1nn$ atoms form a puckered ring around the interstitial [see Fig. 1(b)]. Each unit consisting of one $1nn$ atom and the two $2nn$ atoms it bonds to contains two complete bonds and the two sp^3 orbitals pointing toward the neighboring $1nn$ atoms. Thus, we need a total of six basis states per unit, or 36 basis states for all six units.

The interstitial defect now has lower symmetry than in the tetrahedral case. The coupling of the interstitial with its nearest neighbors was considered exactly, and expressed in terms of all four interactions $V_{ll'm}$. The 40×40 matrix was diagonalized numerically. The resulting levels are either singly degenerate (A) or doubly degenerate (E).

D. Choice of parameters

The on-site energies $E_s^{(a)}$ and $E_p^{(a)}$ were determined from atomic levels. The s energies for Hg and Cd and the p energies for Te and In were obtained from experimental ionization energies,[11] by averaging over all states with the ground-state configuration (s^2, s^2p^4, etc.). The other energies were obtained from the above energies by using estimates of the s–p promotion energy based on Hartree–Fock calculations.[12] The resulting energies were $E_s = -10.43$, -8.99, -18.0, and -11.4 eV and $E_p = -5.0$, -4.77, -7.94, and -5.64 eV for Hg, Cd, Te, and In, respectively.

The off-site parameters were assumed to depend only on the bond length d, and were determined by $V_{ll'm} = \eta_{ll'm}\hbar^2/md^2$ with the tight-binding values $\eta_{ss\sigma} = -1.32$, $\eta_{sp\sigma} = 1.42$, $\eta_{pp\sigma} = 2.22$, and $\eta_{pp\pi} = -0.63$.[13]

III. RESULTS AND DISCUSSION

We obtained the energies of deep levels in the energy-gap region due to In and self-interstitials (Hg, Cd, Te) for CdTe and HgTe. These are shown in Fig. 2. The position of the defect in the lattice is given in parentheses. The occupancy of the neutral interstitial levels, their symmetries, and the corresponding one-electron charge densities on the defect, on all 1 , atoms, and all 2 nn atoms are also indicated.

The position of the valence band (and the energy gap shown for CdTe) was determined by the full sp^3 tight-binding theory, using the same values of $V_{ll'm}$ as in the interstitial calculation. In Fig. 2, we have shown the defect level energies relative to the calculated valence-band edge for CdTe and HgTe. Use of the valence-band edge as the reference level, rather than the conduction-band edge, appears to give good results for the deep levels of the vacancy in several materials, as will be discussed elsewhere.[16] Although the calculated energy gap does not vanish in HgTe, due to the neglect of the spin–orbit interaction, the gap in Fig. 2 is drawn to show the energy gap going to zero as the alloy becomes more Hg rich, as is seen experimentally. The lines between the localized defect levels show schematically the behavior of the levels as we go from CdTe to HgTe.

The levels were analyzed with respect to their localized deep character, to avoid inclusion of quasiextended (or surface) states. In this analysis the following criteria were used to identify localized states. (i) large shift of the energy of the level as compared to bulk, or isolated-defect parent level, (ii) large amount of charge on the defect site, and (iii) significant change of wave function on $1nn$ and $2nn$ atoms as compared with the parent bulk state. Using these criteria, we find that the hexagonal level of Hg at $E = E_v + 1.2$ eV in HgTe loses its localized character in CdTe, and is thus not shown on the CdTe side. Similarly, the hexagonal level of Hg at $E = E_v + 0.9$ eV in CdTe was not recognized as localized on HgTe side.

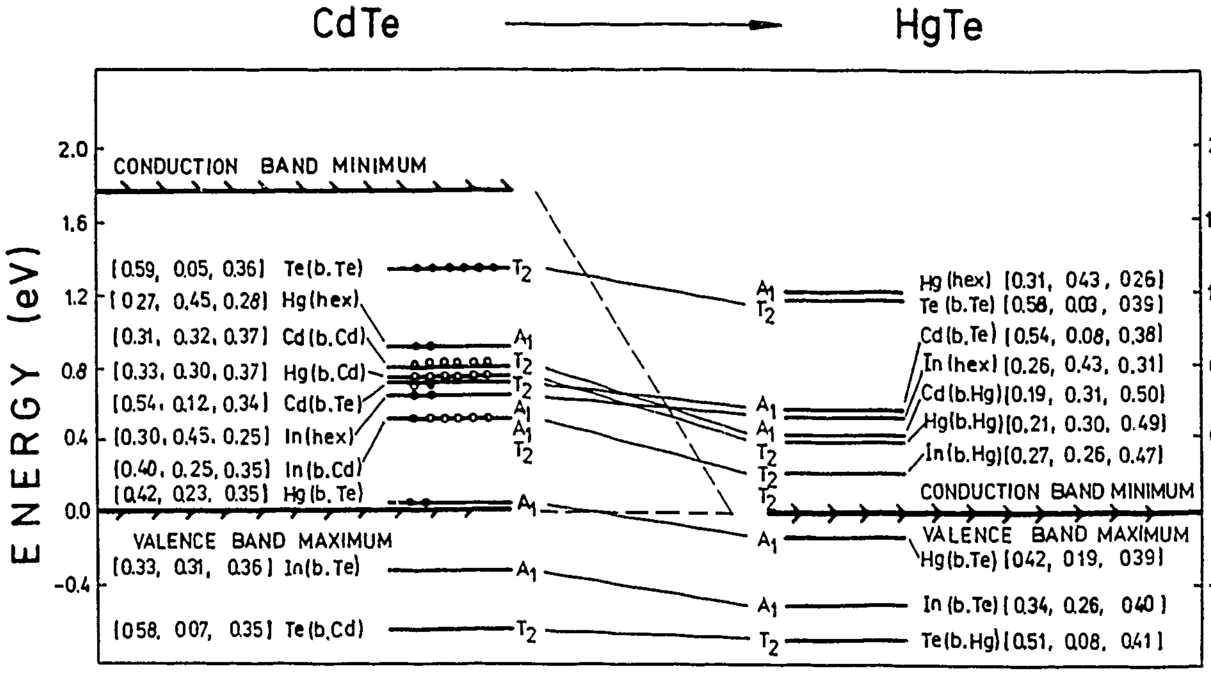
CdTe
HgTe
ENERGY (eV)
2.0
1.6
1.2
0.8
0.4
0.0
-0.4
CONDUCTION BAND MINIMUM
[0.59, 0.05, 0.36] Te(b.Te) T2
[0.27, 0.45, 0.28] Hg(hex)
[0.31, 0.32, 0.37] Cd(b.Cd) A1
[0.33, 0.30, 0.37] Hg(b.Cd) T2
[0.54, 0.12, 0.34] Cd(b.Te) T2
[0.30, 0.45, 0.25] In(hex) A1
[0.40, 0.25, 0.35] In(b.Cd) A1 T2
[0.42, 0.23, 0.35] Hg(b.Te) A1
VALENCE BAND MAXIMUM
[0.33, 0.31, 0.36] In(b.Te) A1
[0.58, 0.07, 0.35] Te(b.Cd) T2
A1 T2
Hg(hex) [0.31, 0.43, 0.26]
Te(b.Te) [0.58, 0.03, 0.39]
Cd(b.Te) [0.54, 0.08, 0.38]
In(hex) [0.26, 0.43, 0.31]
Cd(b.Hg) [0.19, 0.31, 0.50]
Hg(b.Hg) [0.21, 0.30, 0.49]
In(b.Hg) [0.27, 0.26, 0.47]
A1 A1 T2 T2 T2
CONDUCTION BAND MINIMUM
A1
VALENCE BAND MAXIMUM
Hg(b.Te) [0.42, 0.19, 0.39]
A1 In(b.Te) [0.34, 0.26, 0.40]
T2 Te(b.Hg) [0.51, 0.08, 0.41]

FIG 2. The localized levels due to In and self-interstitials in tetrahedral and hexagonal positions in HgCdTe. *X(b. Y)*: tetrahedral level of *X* interstitial located between *Y* atoms; (hex): hexagonal level; *A*, *E*, A_1, T_2: symmetry of the state ●●○○○○. occupany of the state; ●: occupied; ○: empty. [*a,b,c*]: charge densities on *a*, interstitial; *b*, all 1*nn* atoms; *c*, all 2*nn* atoms.

Considering the behavior of the deep levels and their positions in the gap, we first note that the calculated offset of the valence-band edge turns out to be negligible, due to the strong anion character of the valence-band maximum in the sp^3 tight-binding scheme. The change in the band gap is almost entirely accounted for by the lowering of the conduction-band minimum as the concentration of Hg increases. Therefore, the change of the band gap with composition has little effect on the position of the deep levels measured from the valence-band edge. The correct band offset of 0.35 eV[14] may be obtained by including the effects of the *d* electrons[15] However, the corrections to the energies of the deep levels (relative to the valence-band edge) due to *d* electrons should lie within the accuracy of tight-binding calculations such as ours. These calculations are most reliable for characterization of the levels and energy trends, and these are not expected to be affected by the inclusion of *d* states.

The calculated changes in the energy of the deep levels as the concentration of Hg in $Hg_{1-x}Cd_xTe$ is increased result then from the substitution of Hg, instead of Cd, on most of the cation sites in the vicinity of the interstitial. The shifts of the energy levels as we go from CdTe to Hg-rich HgCdTe are not uniform. For tetrahedral interstitials, they are biggest for defects with cation nearest neighbors, and/or a sizable amount of electronic charge on cations. The two T_2-symmetry levels shown for Cd and Hg interstitials satisfy both of these conditions, and thus they exhibit the strongest shift. This leads to the crossing of the levels in the intermediate concentration range.

Considering the self-interstitial levels which could be responsible for the midgap tunneling in $Hg_{0.8}Cd_{0.2}Te$, we find that the A_1-symmetry level of Hg with Te nearest neighbors (with energy $E = E_v + 0.04$ eV in CdTe) appears to be a good candidate. This is in agreement with suggestions which have been made, based on experiment, that Hg interstitials may be a source of the midgap tunneling levels.[2] However, the accuracy of the present calculation is not sufficient to determine whether this A_1 level really lies in the gap for $Hg_{0.8}Cd_{0.2}Te$. The localized state associated with this Hg level has a strong cation character, as more than 70% of the electronic charge is located on cations. Experimental efforts to further characterize the midgap tunneling centers would be very useful in identifying these centers.

Indium doping was found to give rise to two deep levels in the gap region for CdTe. However, neither of them is expected to act as an acceptor level which could lead to signficant self-compensation in CdTe. The hexagonal In level (at $E = E_v + 0.6$ eV in CdTe) is occupied for a neutral interstitial, and thus it cannot serve as an acceptor level The T_2-symmetry tetrahedral level (at $E = E_v + 0.5$ eV) due to In with cation nearest neighbors is partially empty, and in principle it could serve as an acceptor level. However, it seems more likely for In to occupy the tetrahedral position between anions, as it does in substitutional sites. Thus, we believe that tetrahedral In with cation nearest neighbors is energetically less favorable and hence much less numerous than tetrahedral In with anion nearest neighbors. The latter interstitial was found to have only shallow donor levels, as does substitutional In. Therefore, we conclude that In in tetrahedral or hexagonal interstitial positions does not introduce acceptor levels which could account for the electrical inactivity found in MBE-grown In-doped CdTe. The formation energy calculations which are needed for the final confirmation of our assumption concerning the most favorable tetrahedral site are now in progress.[16]

ACKNOWLEDGMENTS

This work was supported in part by the Night Vision and Electro-Optics Laboratories and the ARO under ARO Contract No. DAAL03-87-K-0061 and No. DAAG29-85-K-0119, and by the Institute for Manufacturing Research.

[a)] Permanent address: Institute of Physics, Warsaw Technical University, Koszykowa 75, 00-662 Warszawa, Poland.

[1] C. E. Jones, K. James, J. Merz, R. Braunstein, M. Burd, M. Eetemadi, S. Hutton, and J. Drumheller, J. Vac. Sci. Technol. A 3, 131 (1985).

[2] H. R. Vydyanath (private communication).

[3] R. N. Bicknell, N. C. Giles, and J. F. Schetzina, Appl. Phys. Lett. 49, 1095 (1986).

[4] G. D. Watkins, *Radiation Damage in Semiconductors* (Dunrod, Paris, 1967), p. 97.

[5] See, e.g., M. Lanoo and J. Bourgoin, in *Point Defects in Semiconductors*, edited by M. Cardona (Springer, Berlin, 1981), Vol. 22, p. 68.

[6] M. Lanoo and M. Schlüter, Phys. Rev. B 31, 5468 (1985).

[7] J. C. Slater and G. F. Koster, Phys. Rev. 94, 1498 (1954).

[8] G. D. Watkins and R. P. Messmer, in *Computational Methods for Large Molecules and Localized States in Solids*, edited by F. Herman, A. D. Mclean, and R. K. Nesbet (Plenum, New York, 1973), p. 133.

[9] S. T. Pantelides, in *Defect Complexes in Semiconductor Structures*, edited by J. Giber, F. Beleznay, I. C. Szép, and J. László (Springer, Berlin, 1983), p. 75; and (private communication).

[10] P. Löwdin, Phys. Rev. 19, 1396 (1951).

[11] C. Moore, *Atomic Energy Levels* (National Bureau of Standards, Gaithersburg, MD, 1958).

[12] E. Clementi and C. Roetti, At. Data Nucl. Data Tables 14, 177 (1974).

[13] W. A. Harrison, Phys. Rev. B 27, 3592 (1983).

[14] C. K. Shih and W. E. Spicer, Phys. Rev. Lett. 58, 2549 (1987).

[15] S.-H. Wei and A. Zunger, Phys. Rev. Lett. 59, 144 (1987).

[16] S. Goettig and C. G. Morgan-Pond (to be published).

Interstitial total energies and diffusion barriers in $Hg_{1-x}Cd_xTe$

C. G. Morgan-Pond and J. T. Schick
Department of Physics and Astronomy, Wayne State University, Detroit, Michigan 48202
S. Goettig
Department of Physics and Astronomy, Wayne State University, Detroit, Michigan 48202 and Institute of Physics, Warsaw Technical University, Warsaw, Poland

(Received 11 October 1988; accepted 13 November 1988)

The previous simple model used to calculate energy trends for the deep levels due to localized electronic states associated with interstitial and substitutional defects has been extended to obtain estimates of the total energy for interstitials at different sites in the lattice. These calculations have been applied to predict the preferred tetrahedral site for Hg, Cd, In, and Te interstitials in $Hg_{1-x}Cd_xTe$, and to investigate a possible diffusion path for these interstitials.

I. INTRODUCTION

Both the electronic behavior and the compositional profile resulting from growth or processing of semiconductor alloys can be strongly influenced by the presence of impurity and self-interstitials. Deep levels corresponding to localized interstitial states may lead to electrical activity for interstitials with a sufficiently favorable formation energy to be numerous. Even when other defects are more numerous, interstitials often make a major contribution to the diffusion processes which determine dopant profiles and to chemical interdiffusion in superlattices and junctions. Calculating the total energy of the interstitials at different positions, and the electronic deep levels due to these interstitials, can help broaden our understanding of the contributions of interstitials to electronic behavior and kinetic processes in semiconductors.

Calculations of the localized states due to point defects in semiconductors may be divided into two main categories. Green's function calculations, as have been developed for interstitial defects in Si,[1] account fully for the periodicity of the host crystal. Methods in which a localized basis is separated from the rest of the crystal, or repeated periodically, are only valid when it can be shown that the boundary conditions chosen for the localized basis do not strongly alter the description of the localized states from what would be expected for an isolated defect in an infinite crystal. However, these methods are more easily applicable to problems such as defects with lattice distortions and defects in alloys.

We have previously developed a simple tight-binding model for interstitial and substitutional defects in tetrahedrally bonded semiconductors with significant ionic and metallic character.[2] In this approach, the localized states are described in terms of a small localized basis.[3] For substitutional and high-symmetry (tetrahedral) interstitials, the energy levels and wave functions of the localized states are obtained analytically. Energy levels and wave functions have been obtained numerically for hexagonal interstitials. Although the calculated deep levels cannot be viewed as quantitatively reliable, the general energy-level structure obtained from these simple calculations compares well, with a few exceptions, with self-consistent Green's function and experimental results for interstitials and substitutional defects in Si, GaP, GaAs, and CdTe.[2] Correct symmetries and occupancies are obtained, and known chemical trends reproduced. In this work, we investigate the effects of charge transfer on the deep-level structure, and extend these calculations to obtain estimates of the total energies for interstitials at different sites in the lattice.

While experimental evidence indicates that interstitials may be correlated with the midgap tunneling levels in Hg-rich HgCdTe,[4] reliable identification of specific defect levels in HgCdTe has been a very difficult problem. Previous results of this model for the deep levels due to In and self-interstitials in $Hg_{1-x}Cd_xTe$ alloys have been reported, and implications for self-compensation and doping behavior discussed, assuming that the preferred tetrahedral site for Hg and In interstitials is between anions.[2] Total energies are calculated here for In and Hg self-interstitials at different sites, and the preferred tetrahedral site for each interstitial is determined.

Experimental evidence also indicates that interstitial defects play a major role in cation interdiffusion at CdTe/HgTe junctions.[5] Developing a more accurate picture of interstitials in these materials is therefore as important for understanding diffusion mechanisms as it is for understanding the microscopic structure and properties of defects associated with the midgap levels and other observed electronic levels. Results of the total energy calculations for In and self-interstitials are used to investigate whether the low-electron-density channel which passes alternately through tetrahedral sites between cations and tetrahedral sites between anions is likely to be an important diffusion path for these interstitials in HgCdTe. Possibilities for charge-transfer-assisted diffusion are discussed.

II. LOCAL MATRIX APPROACH

A. Basic model

In this approach, the localized states associated with the defect are described in terms of a small basis of atomic orbitals, localized around the defect. These basis states are decoupled from the rest of the crystal by the method of "soft separation," i.e., without breaking any of the covalent bonds (the strongest coupling in the crystal). The interactions of the interstitial with the rest of the localized basis states are treated exactly, within the two-center tight-binding approximation, while the weaker interactions which couple the local basis to the rest of the crystal are systematically neglected. The effects of the polar, metallic, and covalent coupling within the localized basis are thus included, while preserving the simplicity of the small-basis description.[2]

The minimal basis for the localized interstitial states in this model includes the atomic orbitals on all the nearest neighbors of the interstitial, which are improperly coordinated due to the presence of the defect, and all the sp^3 hybrids on more distant atoms which are involved in bonds with hybrids on the nearest-neighbor atoms. Adding the atomic orbitals on the interstitial atom itself gives a basis of 36 states, composed of atomic orbitals on 15 atoms, for the tetrahedral interstitial, and a basis of 40 states, composed of atomic orbitals on 19 atoms, for the hexagonal interstitial. The analogous basis for substitutional defects contains 32 states, composed of atomic orbitals on 17 atoms. The local structure around each of these defects, including all the atoms which contribute states to the localized basis, is shown in Fig. 1.

The minimal basis is cut off from the rest of the crystal by neglecting the metallic coupling (which is proportional to the promotion energy, $E_p - E_s$) on the atoms bonded to the nearest neighbors, and all the two-center interactions between hybrids on the nearest-neighbor atoms and hybrids on further atoms, except the ionic and covalent coupling between the hybrids on the nearest-neighbor and further atoms which are covalently bonded to each other. This method of separation does not introduce surface states due to dangling bonds or bonds of a different type, such as the host–hydrogen bonds which occur when the bonds at the surface of the local cluster are terminated with hydrogen.

B. Tight-binding parameters and approximations

The deep-level energies and wave functions given by the formulas derived for substitutional defects and tetrahedral interstitials,[2] and found numerically for hexagonal interstitials, depend on the approximations and the tight-binding parameters used to define the matrix elements of the Hamiltonian. Modifications in the set of parameters used will cause some change in the calculated levels. However, recent work on structural total energies for bulk semiconductors[6] has shown that the results of such tight-binding total energy calculations are quite insensitive to modifications, provided that the parameters reflect the chemical trends in the atomic data. In this work, we follow the ideas of Harrison,[7] and assume that the on-site matrix elements are most sensitive to the chemical character of the atom occupying the site, while off-site matrix elements are most sensitive to the interatomic distance.

The on-site energies are determined using atomic orbital energies obtained from experiment, supplemented by Hartree–Fock results where necessary. The first ionization energies taken from x-ray data[8] are used to determine the p-orbital energy E_p for atoms with an occupied p valence shell, and to determine the s-orbital energy E_s for atoms with only s valence electrons (i.e., Hg, Cd). For atoms with only s valence electrons, the average excitation energies are also available from the x-ray data (and are not available from Hartree–Fock calculations), and these are used to determine the promotion energies, $E_p - E_s$. The average excitation energies are generally not available from the experimental data for atoms with occupied p valence shells. Therefore, for these atoms the promotion energy is taken from Hartree–Fock results.[9] The resulting energies for the atoms considered in

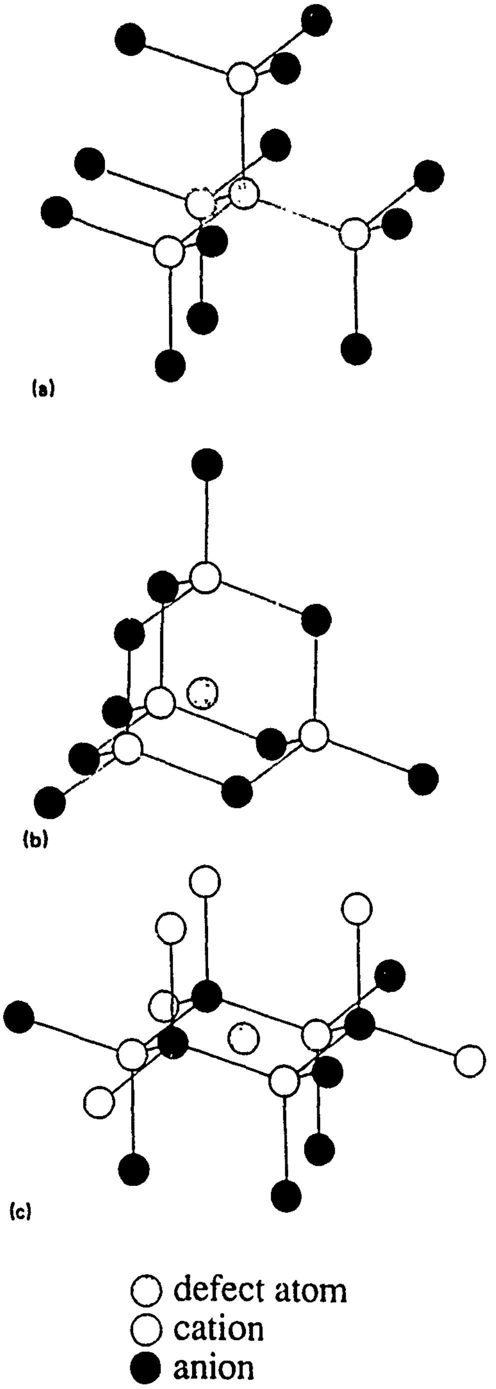

FIG. 1. Atomic structure of the (a) substitutional defect, (b) tetrahedral interstitial, and (c) hexagonal interstitial.

this work are $E_s = -10.43$, -8.99, -18.28, and -10.56 eV and $E_p = -5.00$, -4.77, -9.01, and -5.78 eV for Hg, Cd, Te, and In, respectively.

We use the two-center approximation for the off-site matrix elements, and assume that these matrix elements depend only on the bond length d. Following Harrison,[7] we assume that the matrix elements describing the interaction between nearest-neighbor atoms have the form $V_{ll'm} = \eta_{ll'm}\hbar^2/md^2$, with the tight-binding parameters $\eta_{ss\sigma} = -1.32$, $\eta_{sp\sigma} = 1.42$, $\eta_{pp\sigma} = 2.22$, and $\eta_{pp\pi} = -0.63$, where m is the free-electron mass. Although these coefficients were developed by Harrison to describe the interactions between atoms in perfect tetrahedrally bonded crystals, we assume that the interaction between the interstitial and the host atoms has the same dependence on d, and may be described by the same set of parameters.

The tight binding band structure obtained for perfect crystals has often been improved by adding an excited s^* orbital[7,10] or small next-nearest-neighbor interactions,[9] which could be included in the present small-basis model. We would like to treat the chemical trends and the bonding for host and interstitial atoms on the same footing. However, the justification for including an s^* orbital or second-nearest-neighbor interactions for the interstitial, using parameters fit to the bulk band structure, is not obvious. Therefore, we use only nearest-neighbor interactions in the present work.

III. CHARGE TRANSFER EFFECTS

We note that the effective intra-atomic repulsion for charge transfer between cations and anions in the perfect crystal is close to zero for the materials considered, as discussed in detail by Harrison.[11] We therefore neglect the effect of charge transfer on the on-site matrix elements for the atoms in the perfect crystal. When the interstitial is introduced, additional charge transfer between the interstitial and the host atoms occurs. The effects of this charge transfer to or from the interstitial should be greatest on the interstitial itself.

We estimate the effects of this charge transfer by introducing an effective intra-atomic Coulomb repulsion between electrons on the intersitital. The Coulomb shift resulting from removal of an electron from the interstitial atom to an infinite distance, $-U$, is obtained from the difference of the first and second ionization energies for this atom, taken from x-ray data.[8] In the case of In, where the first electron is removed from the p shell, and the second from the s shell, U is obtained from x-ray data,[8] as is done for all other interstitial atoms. However, the difference between the first and second ionization energies for In is not equal to $-U$, but to $E_s - E_p - U$. In these calculations, charge transferred from the neutral interstitial is not removed to an infinite distance, but is tranferred to the nearest neighbors of the interstitial, at a distance of d_0, or to atoms bonded to the nearest neighbors, which are not much further away. Therefore, the effective Coulomb shift resulting from transfer of an electron between the interstitial and nearby host atoms is given by $U_{\rm eff} = U - 14.4\ eV\,(\text{Å}/d_0)$.

After the Hamiltonian matrix is diagonalized to obtain the deep-level energies and the wave functions of the localized states, the shift in the on-site energy for the interstitial due to charge transfer to the surrounding atoms is calculated, and the new Hamiltonian matrix, including this energy shift, is diagonalized. This procedure is repeated until a self-consistent solution is reached. The resulting charge on the interstitial itself, before the defect becomes ionized, is shown in Table I for various interstitials at different sites in CdTe and Hg-rich HgCdTe. Interstititals in the tetrahedral position between cations (T1), where the electron density is low, tend to lose some electronic charge to the surrounding atoms. Interstitials in the tetrahedral position between anions (T2), where the electron density is higher, tend to gain some electonic charge from their neighbors. These charge transfers are on the order of 25% of an electron. Interstitials in the hexagonal position, which have an equal number of cation and anion nearest neighbors, tend to have much smaller charge transfers. The preferred ionization states for these interstitials, assuming a Fermi level near the middle of the gap, are also listed in Table I. Interstitials in the T1 position, in the region of low electron density, tend to remain neutral or become negatively charged, while interstitials in the T2 and hexagonal positions tend to become positively charged.

The shifts in the deep-level energies for neutral interstitials due to charge transfer are on the order of 0.4 eV for tetrahedral interstitials, and 0.05 eV for hexagonal interstitials. The effects of charge transfer do not change the qualitative conclusions reported earlier.[2] There is still a level of A_1 symmetry in the vicinity of the gap, due to Hg interstitials in the T2 position. This level is of interest, since it has been suggested[4] that the midgap tunneling levels in Hg-rich HgCdTe are associated with Hg interstitials. If the T2 position for Hg interstitials is preferred, it is certainly possible that the midgap tunneling levels of Hg-rich HgCdTe are due

TABLE I. Charge on interstitials.

Material	Interstitial	Position	Preferred charge state	Net charge on interstitial before ionization (units of e)
CdTe	Cd	T1[a]	Cd^0	+0.3
		H[b]	Cd^{++}	0.
		T2	Cd^{++}	−0.3
	In	T1	In^0	−0.4
		H	In^{++}	−0.1
		T2	In^{+}	−0.2
	Te	T1	Te	−0.3
		H	Te^{++}	0.
		T2	Te^{++}	−0.1
Hg rich HgCdTe	Hg	T1	Hg^0	−0.2
		H	Hg^{++}	−0.3
		T2	Hg^{++}	−0.2

[a] T1 ≡ tetrahedral position between cations.

[b] H ≡ hexagonal position.

T2 ≡ tetrahedral position between anions.

to T2 Hg interstitials, perhaps associated with another defect or complex which pulls this level into the gap.

The deep-level energies for the In interstitial in the T2 position are not strongly affected by charge transfer, and any shifts which do result from charge transfer in this case only tend to make the T2 In interstitial an even stronger donor. Therefore, as previously discussed,[2] if the T2 position is preferred for the In interstitial, we do not expect self-compensation in In-doped HgCdTe due to isolated In interstitials. The electrical inactivity which is often observed in In-doped CdTe films grown by MBE without laser illumination[12] must result from the failure of the In to occupy isolated substitutional sites, or compensation of the shallow substitutional donors by some other defects.

IV. OVERLAP AND TOTAL ENERGY

In order to calculate total energies, the short-range repulsion arising from overlap of the electron wave functions centered on neighboring atoms must be included. The overlap was assumed to be proportional to the hopping matrix element divided by the average on-site energy, and to have the form assumed by Majewski and Vogl[6]:

$$S_{ll'm} = \frac{1}{K_{AB}}\left[\frac{2}{E_{lA} + E_{l'B}}\right]\frac{\eta_{ll'm}\hbar^2 r_0}{md^3},$$

where E_{lA} is the atomic orbital energy for orbital l on atom A, and r_0 is an average orbital radius determined from the Coulomb repulsion energy of two electrons on the same atom (U_A for atom A):

$$r_0 = \frac{e^2}{2}\left[\frac{1}{U_A} + \frac{1}{U_B}\right].$$

K_{AB} is a scaling constant close to 1, which depends on the row of the Periodic Table containing A and B. For A and B from different rows, K_{AB} is given by the geometric average. Since we use values for the atomic-orbital energies and for U determined from experiment, and Harrison's tight-binding parameters, $\eta_{ll'm}$, while Majewski and Vogl use Hartree–Fock results for the orbital energies, values obtained from Harrison's universal parameter theory for U, and a slightly different set of tight-binding parameters, we have determined the values of K appropriate for our set of parameters by fitting to the equilibrium lattice constants for Si, C [illegible] and Sn. This procedure gives us values for K which are $\frac{3}{4}$ of the values of Majewski and Vogl.

If we approximately orthogonalize the localized basis functions, taking into account their overlap to first order, we will get corrections to both the off-site and the on-site matrix elements of the Hamiltonian. However, since the off-site matrix elements were constructed empirically, they should already include the effects of overlap. The shifts in atomic-orbial energies resulting from overlap are typically the same, to within ± 30%, for all the orbitals in the minimal basis for a particular interstitial defect. Therefore, we have taken the effect of overlap to be a constant energy shift equal to the average energy shift for the occupied orbitals in the minimal basis for each defect.

The total energy for a semiconductor, with or without an interstitial defect, is given by

$$E_{\text{tot}} = \sum_{n}^{\text{occ}} \epsilon_n - E_{ee} + E_{\text{core-core}},$$

where the sum of electron energies ϵ_n is over the occupied one-electron states, the electron–electron interactions (which have been included twice in the first term) are subtracted out, and the core–core interactions are added. If the material is composed of spherically symmetric, neutral atoms with no overlap of charge densities, the last two terms cancel.

We may assume that these two terms cancel for the materials we are considering, in the absence of charge transfer. When electrons are transferred and the atoms become charged, the electron–electron interaction energy changes. In setting up the Hamiltonian to solve for the one-electron energy levels ϵ_n, we have assumed that the only change in the electron–electron interaction energy which occurs as a result of charge transfer is due to the effective Coulomb repulsion which opposes the transfer of more electrons to the interstitial from its immediate vicinity. When the electronic charge on the interstitial changes from the number of valence electrons on the neutral atom Z_I, to Q_I, the resulting change in the electron–electron interaction energy is $U_{\text{eff}}(Q_I^2 - Z_I^2)/2$, which must be subtracted from the sum of the energies of the occupied one-electron states to give the total energy.

Effects of relaxation and lattice distortion have been neglected. If relaxation of the lattice is allowed, the total energies may be modified. However, lattice relaxation is expected to be less important for tetrahedral interstitials than for interstitials at sites with lower symmetry and less favorable nearest-neighbor distances. Therefore, inclusion of these effects shold not change the trends discussed in the present work.

We report here the total energies of the localized basis, containing a neutral interstitial defect, relative to the total energy of the localized basis with no interstitial, plus the isolated interstitial atom at an infinite distance. The total energies obtained from this model are not expected to be quantitatively accurate, but provide estimates useful for indicating the preferred position of interstitials, and studying trends in the barriers to interstitial diffusion along different paths. Using the same approximations for the total energy as described above, we obtain calculated values for the cohesive energy of 1.4 eV/bond for both CdTe and HgTe, which may be compared with the experimental values of 1.1 eV/bond (CdTe) and 0.8 eV/bond (HgTe). The bonding energy is overestimated in HgTe, due to neglect of the effect of the d states on the bonding.

V. PREFERRED INTERSTITIAL SITES

Total energy differences for selected interstitials at different sites in the lattice are given in Table II. $\tilde{E}^0_{T1} - \tilde{E}^0_{T2}$ is the difference of the total energies for the neutral interstitial in the T1 and T2 tetrahedral positions, requiring all bound electrons or holes to be in localized deep levels or resonances. $E^0_{T1} - E^0_{T2}$ is the difference of the total energies for the neutral interstitial in the T1 and T2 tetrahedral positions, allowing for the formation of shallow hydrogenic donor or accep-

TABLE II. Interstitial total energies.[a]

Material	Interstitial	$\tilde{E}^0_{T1} - \tilde{E}^0_{T2}$ (eV)	$E^0_{T1} - E^0_{T2}$ (eV)	$E_{T1} - E_{T2}$ (eV)	Preferred transition
CdTe	Cd	$+6.4$	$+7.7$	$+10.9 - 2\mu$	$Cd^0_{T1} \to Cd^{+2}_{T2}$
	In	$+1.3$	$+3.2$	$+4.8 - \mu$	$In^0_{T1} \to In^{+}_{T2}$
	Te	-1.8	(-3.5)[b]	$(+2.9 - 6\mu)$[b]	$Te^{-2}_{T1} \to Te^{+4}_{T2}$
Hg rich HgCdTe	Hg	-1.8	$+1.2$	$+1.4 - 2\mu$	$Hg^0_{T1} \to Hg^{+2}_{T2}$

[a] T1 ≡ tetrahedral position between cations. T2 ≡ tetrahedral position between anions. $\tilde{E}^0$ ≡ total energy for neutral interstitial with all electrons in localized deep levels or resonances. E^0 = total energy for neutral interstitial allowing shallow donor/acceptor levels. E ≡ total energy for preferred charge state. μ ≡ Fermi level, measured from the valence-band edge.

[b] Not accurate due to large charge transfer.

tor levels, so that bound electrons or holes may occupy these hydrogenic states, with energies near the band edge, rather than deep localized states with energies outside the gap. $E_{T1} - E_{T2}$ is the difference of the total energies for interstitials in the preferred ionization state, listed in Table I, for T1 and T2 tetrahedral positions. The deep-level structure obtained in these self-consistent calculations for neutral interstitials does not provide a good representation for highly ionized interstitials, due to the large charge transfer. For this reason, we have listed the total energy differences between Te interstitials in T1 and T2 positions in parentheses, when the many holes and electrons in deep resonant states have been allowed to fall to shallow hydrogenic bound states, or the interstitials have ionized to their preferred charge state.

As shown in Table I, the calculated total energy for neutral indium interstitials is higher in the tetrahedral position between cations (T1) than in the tetrahedral position between anions (T2) by ~3 eV in CdTe. The preferred charge state of these interstitials depends on the Fermi level μ, but for a Fermi level of ~ 1 eV, measured from the valence-band edge, the preferred charge state is neutral, for the T1 In interstitial, and + 1 for the T2 In interstitial. Since the T2 interstitial has an even lower energy when it ionizes to In^+, the total energy difference between T1 and T2 In interstitials in their preferred charge states is even greater than for neutral interstitials. These results support our earlier assumptions[2] that the preferred tetrahedral site for In interstitials is T2. Therefore, although T1 In interstitials have a partially filled deep level in the gap and could potentially serve as acceptors,[2] these interstitials will not be numerous enough to account for the electrical compensation which is seen in non-laser-assisted MBE-grown films of CdTe.[12]

Vydyanath has looked at the effect of Hg overpressures on the midgap tunneling centers in Hg-rich HgCdTe, and suggests these centers may be due to Hg interstitials.[4] We have previously found that the T2 Hg interstitial has an A_1 level in the gap region.[2] In this work, we find that the total energy is lower for Hg interstitials in T2 than in T1 sites. The energy difference is ~ 1 eV for neutral interstitials, and slightly more when the T2 interstitial ionizes to Hg^{+2}. The total energy differences listed for Hg-rich HgCdTe in Table II are for material with a band gap of 0.1 eV, and a Fermi level μ ~0.05 eV. According to these results, tetrahedral Hg interstitials will tend to sit in T2 sites, and contribute A_1 electronic levels in the vicinity of the gap.

The total energy differences listed in Table II for Cd and Te interstitials in CdTe follow the same general trend as was verified above for Hg and In interstitials. elements which sit primarily on cation substitutional sites will prefer the tetrahedral interstitial position on the alternate cation sublattice, and elements which sit primarily on anion lattice sites will prefer the tetrahedral position on the alternate anion sublattice. We find that the T2 position (between anions) is preferred for tetrahedral Cd interstitials, while the T1 position (between cations) is preferred for tetrahedral Te interstitials.

VI. DIFFUSION

Total energy differences for interstitials at different sites can provide useful estimates of diffusion barriers, and help identify probable paths for interstitial diffusion. If one of the tetrahedral sites is the preferred interstitial position, the path through the channels of low electron density, passing alternately through T1 and T2 tetrahedral sites, may be an important avenue for diffusion. We may begin to investigate diffusion barriers along this path by examining the energy differences for interstitials in T1 and T2 sites.

Experimental studies in both CdTe and $Hg_{0.8}Cd_{0.2}Te$ suggest that interstitials play an important role in cation diffusion, and that Cd interstitials in particular play an important role in interdiffusion at HgTe/CdTe junctions.[5] The calculated total energy difference for neutral Cd interstitials in T1 and T2 positions in CdTe, shown in Table II, is ~8 eV, much higher than experimental activation energies.[5] Simple interstitial diffusion through the low-electron-density channel which passes alternately through T2 and T1 sites therefore seems unlikely for Cd.

Calculated total energy differences for neutral interstitials in T1 and T2 positions are ~3 eV for In in CdTe and ~1 eV for Hg in Hg-rich HgCdTe. Although the energy difference is not so great for In interstitials as for Cd interstitials in CdTe, the open channel between T1 and T2 tetrahedral positions also appears to be unlikely for In diffusion. However, this channel appears to be a good candidate for diffusion of Hg in Hg-rich HgCdTe, provided that the energy required to pass through the hexagonal site between tetrahedral sites is

B-6

not excessive. A reliable estimate of the energy required for Hg to pass through the hexagonal site may require the inclusion of relaxation outward of the nearest neighbors of the interstitial, which is beyond the scope of these small-basis calculations.

Diffusion behavior may be quite different for interstitials which are not neutral. As shown in Table I, the preferred charge state for all the interstitials listed changes radically at different sites. Cation interstitials in HgCdTe tend to be neutral in T1 sites, and + 2 in T2 sites and hexagonal sites. In interstitials tend to be neutral in T1 sites and + 1 to + 3 in hexagonal and T2 sites. Anion interstitials tend to be − 2 in T1 sites and + 2 to + 4 in T2 and hexagonal sites. This suggests that the alternating capture and release of charge carriers by interstitials may be important in lowering energy barriers for interstitial diffusion in these materials. If interstitials are allowed to change to their preferred charge state at each site, the diffusion barriers become dependent on the Fermi level. However, the conclusions stated above are not changed: the open channel between interstitial sites appears to be a favorable diffusion path for Hg, less favorable for In, and quite unfavorable for Cd.

VII. CONCLUSION

The small-basis approach previously developed to study trends in the deep-level energies for interstitial and substitutional defects has been extended to include the effects of charge transfer and overlap. Estimates of the total energies of interstitial defects in the tetrahedral position between cations and the tetrahedral psotion between anions are calculated within this model. The preferred tetrahedral site is found to be between cations for Te, and between anions for Cd, Hg, and In. Therefore, as previously suggested,[2] the potential acceptor level calculated within this model for tetrahedral In interstitials between cations should not be important in producing the electrical compensation often observed in In-doped CdTe.[12]

Diffusion along the open channel between tetrahedral sites is found to be unfavorable for Cd and probably unfavorable for In in CdTe, but may be important for Hg in Hg-rich HgCdTe. Charge carrier capture is predicted to lower diffusion barriers for all these interstitials.

ACKNOWLEDGMENTS

This work was supported by the Night Vision and Electro-Optics Laboratories and the ARO under ARO Grants No. DAAL03-87-K-0061 and No. DAAG29-85-K-0119, and by the Institute for Manufacturing Research.

[1] O. F Sankey and J. D. Dow, Phys. Rev. B 27, 7641 (1983).

S. Goettig and C. G. Morgan-Pond, J. Vac. Sci. Technol. A 6, 2670 (1988), S Goettig and C G Morgan-Pond, in Proceedings of the 15th International Conference on Defects in Semiconductors, 1988 (to be published).

[3] S. T. Pantelides, in *Defects in Semiconductors*, edited by J. Giber *et al.* (Springer, Berlin, 1983), p. 75.

[4] H. R. Vydyanath (private communication).

[5] M.-F. S. Tang and D. A. Stevenson, Appl. Phys. Lett. 50, 1272 (1987), and further references cited in this paper.

[6] J. A. Majewski and P. Vogl, Phys. Rev. B 35, 9666 (1987).

[7] W. A. Harrison, Phys. Rev. B 27, 3592 (1983).

[8] C. Moore, *Atomic Energy Levels* (National Institute of Standards and Technology, Gaithersburg, MD, 1958).

[9] E. Clementi and C. Roetti, At. Data Nucl. Data Tables 14, 177 (1974).

[10] P. Vogl, H. P. Hjalmarson, and J. D. Dow, J. Phys. Chem. Solids 44, 365 (1983).

[11] W. A. Harrison, Phys. Rev. B 31, 2121 (1985).

[12] R. N. Bicknell, N. C. Giles, and J. F. Schetzina, Appl. Phys. Lett. 49, 1095 (1986).

Point defects with lattice distortion in CdTe and HgCdTe

J. T. Schick and C. G. Morgan-Pond
Department of Physics and Astronomy, Wayne State University, Detroit, Michigan 48202

(Received 4 October 1989; accepted 29 October 1989)

Results of self-consistent, tight-binding supercell calculations of electronic defect levels and relaxation about defects for As, Sb, and Te interstitials in CdTe and for the Hg vacancy in HgTe are presented. Trends in the localized defect levels and the relaxation of the lattice seen for these defects and for Cd, Hg, and In interstitials, from previous calculations,[1] are discussed. Te interstitials are found to have the largest lattice relaxation of these interstitials in their preferred tetrahedral positions. This may help explain the tendency for excess Te to condense into second-phase inclusions. It is also suggested that a strain-mediated interaction between Te interstitials and cation vacancies may promote the creation of Te antisites in Te-rich HgCdTe.

I. INTRODUCTION

A great deal of attention has been focused on the formation of defects and their effects on semiconductor devices. Defects and defect complexes can fundamentally affect the electronic properties of the crystal. In addition, diffusion of the defects in the material during growth has a profound effect on the uniformity of the crystal. Even at room temperature, defect diffusion may play a significant role in the stability of a crystal over time.

Technologically important defects may be in the form of simple point defects, such as interstitials or vacancies, or may be more extensive. Lattice relaxation occurs for simple point defects as well as for more extended defects, which may involve substantial lattice distortion. This relaxation may change the symmetry of the defect site, and generally does change the charge distribution in the vicinity of the defect, modifying both the defect level energies and the corresponding localized defect states. The resulting strains in the lattice may affect the attraction and binding of point defects into a complex, or to extended defects.

Both experimental evidence[2] and theoretical estimates of diffusion barriers[3] indicate that Hg interstitials may diffuse easily along the open channels between tetrahedral sites in $Hg_{1-x}Cd_xTe$, while Cd interstitial diffusion requires a more complicated process, involving interchanges with atoms on lattice sites. Ultimately, calculation of total energies for highly distorted local configurations may be necessary in order to identify favorable paths for Cd diffusion.

First principles techniques have often been used to calculate the properties of simple defects with only a few degrees of freedom. For example, pseudopotential density-functional approaches[4] and self-consistent Green's function methods[5] have been applied with reasonable success for tetrahedral and hexagonal self-interstitials in silicon. While these methods produce the most reliable results, they require copious amounts of computer time, which is undesirable when the number of problems to study is large, or when many degrees of freedom must be included in order to find the preferred configuration of the lattice surrounding a defect. Tight-binding theory offers an attractive alternative to first principles methods because of the reduced computational effort. Transferability of the parameters to systems other than perfect crystals has been demonstrated by Chadi[6] in his work on surfaces of group IV and III-V semiconductors, and by Tománek[7] in his work on Si clusters. Comparison of tight-binding results to the results of first principles methods[4,5] for interstitials has been encouraging.[8]

We have recently developed a supercell approach for the calculation of total energies in systems with point defects, based on the tight-binding model of Majewski and Vogl,[9] and have applied this technique to self-interstitials in Si[8] and Cd, Hg, and In interstitials in CdTe and HgTe.[1] Lattice relaxation is included, and charge transfer is treated in a fully self-consistent manner. We report here the results of our studies of the properties of As, Sb, and Te interstitials in CdTe and of the Hg vacancy in HgTe, and expand our investigation of trends in the electronic levels and relaxation associated with cation and anion self-interstitials and dopant interstitials in $Hg_{1-x}Cd_xTe$.

II. THEORY AND PARAMETERS

The supercells used in this work have a cubic symmetry, with a side length equal to twice the lattice constant of the crystal. There are 64 atoms in the bulk crystal supercell, one more for interstitials, and one less for vacancies. Only s and p electronic states are considered to participate in the bonding for CdTe and HgTe. In this lattice, an interstitial may be placed at a tetrahedral position, with four anion (or cation) nearest neighbors and six cation (or anion) next nearest neighbors only slightly further away. The hexagonal position, which is at the narrowest passage between two adjacent tetrahedral points, is surrounded by a puckered ring consisting of three anions and three cations. A modified form of Majewski and Vogl's[9] energy formalism is used to predict the most favorable configuration of the neighboring atoms. We permit a breathing mode of relaxation of the nearest neighbor atoms radially toward or away from the defect, and a change in puckering of the nearest neighbor ring for the hexagonal interstitials. At this time we have not yet included Jahn–Teller distortions, which are expected for the neutral states of the cation vacancy and Te and dopant interstitials, where partially occupied degenerate states occur. Jahn–Teller distortion will not occur for charge states with completely filled or empty defect levels, such as the doubly charged cation vacancy in HgCdTe.

0734-2101/90/021108-04$01.00 © 1990 American Vacuum Society

The interactions are given by Harrison's inverse square tight-binding form[10]

$$t_{ll'm} = \eta_{ll'm} \frac{\hbar^2}{md^2}, \tag{1}$$

where d is the separation between the interacting atoms, m is the mass of the electron and $\eta_{ll'm}$ is a "universal" parameter for the interaction between the l and l' orbitals in a bond of m symmetry. We impose a cutoff of 1.39 times the nearest neighbor distance in the bulk crystal, which corresponds to including only first neighbor interactions in the bulk crystal and with the hexagonal interstitial, and first and second neighbor interactions with the tetrahedral interstitial.

The on-site energies as expressed by Majewski and Vogl[9] are given by

$$\epsilon_{\lambda i} = w_{\lambda i} - U_i(Z_i - Q_i) - \sum_{i'(\neq i)} (Z_{i'} - Q_{i'}) V(\mathbf{R}_i - \mathbf{R}_{i'}) + f_{\lambda i}, \tag{2}$$

where $w_{\lambda i}$ is the energy of the λ orbital of the isolated, neutral atom on site i. As the charge is redistributed in ionic crystals and crystals with defects, corrections to the one electron potential resulting from this charge transfer are included. The quantity $(Z_i - Q_i)$ represents the electron deficiency on the atom at site i, where Z is the valence of the neutral atom and Q is the number of electrons at the site. The second term is the intra-atomic correction, and the third term is the interatomic correction. U_i is the average Coulomb repulsion between two electrons on the same atom.[11] The modified Coulomb potential, used in the third term to account for the fact that at small separations the distinction between intra-atomic and interatomic is meaningless, is given by[10]

$$V(\mathbf{R}_i - \mathbf{R}_{i'}) = \frac{e^2}{|\mathbf{R}_i - \mathbf{R}_{i'}|}\left[1 - \exp\left(-\frac{\overline{U}|\mathbf{R}_i - \mathbf{R}_{i'}|}{e^2}\right)\right], \tag{3}$$

where e is the charge of the electron and $\overline{U}$ is the average Coulomb repulsion for the atoms in the crystal. This potential goes to $\overline{U}$ as the distance between neighboring atomic sites becomes small, while for large separations it becomes Coulombic. The summations are carried out for the third term using Ewald's method.[12] Since the on-site energies depend explicitly on the distribution of charge in the crystal, it is necessary to iterate until a self-consistent solution for the eigenstates of the system is found.

The overlap correction $f_{\lambda i}$ provides the repulsion necessary to prevent the crystal from collapsing. Including effects of nonorthogonality to first order in the overlap S this correction is $f_{\lambda i} = -\frac{1}{2}(SH_{\rm el} + H_{\rm el}S)_{\lambda i,\lambda i}$, where $H_{\rm el}$ is the one electron Hamiltonian made up of the interactions and on-site energies described above[9] The overlap between orbital l on atom A and orbital l' on atom B is[9,11]

$$S_{ll'm} = \eta_{ll'm} \frac{2}{K(w_{lA} + w_{l'B})} \frac{\hbar^2 r_0}{md^3}, \tag{4}$$

where K is a numerical constant close to one, and r_0 is the average radius of a valence state determined from the Coulomb repulsions U on atoms A and B.

The total energy of the crystal (per supercell) is given by the sum of the one electron energies of the occupied states, corrected for the double counting of the electron–electron interactions, plus a contribution due to interactions between the rigid cores

$$E_{\rm total} = \sum_{n,\mathbf{k}}^{\rm occ} \epsilon_{n,\mathbf{k}} - E_{\rm el\text{-}el} + E_{\rm core\text{-}core}. \tag{5}$$

The electron–electron energy may be separated into two parts

$$E_{\rm el\text{-}el}^{\rm intra} = \frac{1}{2}\sum_{i}^{\rm cell} U_i Q_i^2, \tag{6}$$

$$E_{\rm core\text{-}core} - E_{\rm el\text{-}el}^{\rm inter} = \frac{1}{2}\sum_{i}^{\rm cell} (Z_i + Q_i) \times \sum_{i'(\neq i)}^{\rm crystal} (Z_{i'} - Q_{i'}) V(R_i - R_{i'}). \tag{7}$$

The second summation in Eq. (7) is the same as that in Eq. (2), and therefore is evaluated in the same way. The remaining sums in Eqs. (6) and (7) involve only the atomic sites within the supercell.

Harrison's parameters[10] $\eta_{ss\sigma} = -1.40$, $\eta_{pp\sigma} = 3.24$, $\eta_{pp\pi} = -0.81$, and $\eta_{sp\sigma} = 1.84$ were used for the interactions. Separately defined interactions with more distant neighbors are not included in our current calculations. These interactions are usually small,[9] and cannot be transferred unambiguously to calculations involving interstitials.

The bare atomic s-orbital energies and occupied p-orbital energies are obtained from Hartree–Fock calculations,[14] with the exception of Hg, for which we use Dirac–Fock energies[15] The excited p-level energies are obtained from experimental spectra.[16] The energies are, in eV, $\epsilon_s = -7.20$, -8.93, -10.14, -15.83, -18.66, and -19.06 and $\epsilon_p = -2.99$, -3.50, -5.37, -9.10, -10.05, and -9.79 for Cd, Hg, In, Sb, As, and Te, respectively. The values of K and the d^{-3} dependence of the overlap S were determined by Majewski and Vogl to give the best agreement with the bond lengths, bulk moduli, and preferred crystal structures for a wide variety of insulators and semiconductors.[9] For the row including Cd, In, Sb, and Te, $K = 1.05$, for the As row, $K = 1.16$, and for the Hg row, $K = 0.93$. K is given by the geometric average for overlaps between atoms in different rows. Finally, the values of the intra-atomic Coulomb repulsions, determined by Harrison from experiment,[11] are (in eV) 7.33, 6.95, 6.00, 7.39, 8.31, and 8.00 for Hg, Cd, In, Sb, As, and Te, respectively.

III. INTERSTITIAL AND VACANCY LOCALIZED STATES

Although numerical predictions of deep defect level energies obtained using tight-binding methods are not quantitatively reliable, the general energy level structure obtained from simple tight-binding calculations using a small-basis "local matrix" method compares well, in most cases, with experimental and self-consistent Green's function results for interstitial and substitutional defects in CdTe, GaAs, GaP, and Si.[17] In this work, in addition to a more complete treatment of overlap and charge transfer, we include the coupling of the local matrix describing the defect to the rest of the infinite matrix, by considering a periodic array of defects. To determine the effect of the supercell on the localized states, the dispersion of these states along the [100] and [111] directions was calculated. The dispersion is on the order of 0.05 eV, except for the localized defect states close to the band edges, which often interact strongly with bulk states. The resulting states are of mixed character, less localized on the interstitial and showing some of the larger dispersion expected for bulk states at the band edge. Dispersions for these states can be up to 0.2 eV. In a few of these cases, involving strong interactions between bulk states and localized defect states of similar energy, it appears that the localized character shifts between different states as we move away from the Γ point toward the zone edge. It therefore appears that the uncertainty in deep defect level energies resulting from the use of the supercell approach is less than the uncertainty due to problems inherent in the tight-binding model.

Results for the deep level structure associated with the interstitials of different cation-like atoms, such as Cd, Hg, and In, which prefer to sit on cation sites as substitutional impurities, follow a basic pattern. Cd interstitials in the preferred tetrahedral position (with Te nearest neighbors) in CdTe have a defect level of A_1 symmetry close to the conduction band edge. There is a similar level of A symmetry, roughly resonant with the conduction band edge, for the hexagonal Cd interstitial, and a comparable A_1 level for the tetrahedral Cd interstitial with cation nearest neighbors. The A_1 level for the tetrahedral Hg interstitial with Te nearest neighbors is somewhat lower in energy, and this level moves downward as the composition of the crystal is varied from CdTe to HgTe. For both Hg and Cd interstitials, the A_1 level holds the last two electrons for the neutral interstitial. For Hg and Cd interstitials in the preferred tetrahedral position, relaxation of the lattice around the interstitial allows this level to become more localized on the interstitial itself, and to move slightly lower in the gap. The A_1 level of the tetrahedral In interstitial with Te nearest neighbors falls still lower in the gap, and this interstitial also has a T_2 resonance well above the conduction band edge, which donates an electron into the conduction band.

For interstitials of anion-like atoms, such as Te, As, and Sb, which prefer to sit on anion sites as substitutional impurities in the absence of strong deviations from stoichiometry, a similar trend is observed in the positions of the localized states, paralleling the trend in the atomic levels of the isolated interstitial atoms. For the Sb interstitial between cations in CdTe, there is a partially occupied localized state of T_2 symmetry high in the gap, and an A_1 state close to the valence band edge. The T_2 level for the As interstitial between cations is slightly lower, and the localized A_1 state is now a resonance below the valence band edge. For the Te tetrahedral interstitial between cations, the partially occupied T_2 state in the upper part of the gap and the A_1 resonance just inside the valence band are again slightly lower.

The vacancy is modeled as an atom with an s level at 3000 eV and a p level at 12 000 eV, which is substituted for one of the atoms in the bulk lattice. Because of the range of the atomic energies involved, results for vacancy total energy calculations suffer from an increased level of computational error resulting in an increase in the number of iterations needed to obtain self-consistency. For the Hg vacancy in HgTe, a localized state of T_2 symmetry, with over half of its density on the first neighbors of the vacancy, is found near the valence band edge. Slightly lower in energy is a state of A_1 symmetry, which is even more strongly localized on the nearest neighbors of the vacancy. Similar localized states of A_1 and T_2 symmetry are expected to be near the valence band edge in Hg-rich HgCdTe.

IV. RELAXATION

When the lattice surrounding the defect is allowed to relax, the nearest neighbors of the interstitial move outward, and the nearest neighbors of the vacancy move inward, reducing the size of the hole left at the vacant site. The on-site energies on the interstitial atom, and often on the nearest neighbors of the defect as well, are reduced as the overlap decreases. This allows electronic charge to flow into the defect region.

For interstitial defects, the average distance between the nearest neighbors and the atoms further out, to which they are bonded, decreases as the nearest neighbors relax outward. This increases the covalent coupling and the charge transfer from cations to anions in bonds between the nearest neighbors and atoms further out. In order to minimize fluctuations due to this charge transfer between anions and cations, we have defined an interstitial region consisting of the interstitial and the neighboring atoms which are close enough interact directly with the interstitial (i.e., the first and second neighbor shell for tetrahedral interstitials, and the first neighbor shell for hexagonal interstitials).[1] This region contains both anion and cation neighbors. The net amount of charge transferred into the interstitial region when the lattice is allowed to relax is shown in Fig. 1 for all tetrahedral interstitials. The radial relaxation outward is given in this figure as the fractional change in the interstitial-nearest neighbor distance d. A clear correlation between the amount of charge transferred and the preferred amount of relaxation can be seen. For the hexagonal Cd interstitial in CdTe, a 5.3% increase in puckering of the ring of nearest neighbors is allowed, in addition to the preferred 6.3% radial relaxation of the nearest neighbors outward,[1] resulting in a larger charge transfer of 0.25 electrons into the interstitial region. For the cation vacancy in HgTe, there is also a small charge transfer (~0.02 electrons) onto the nearest neighbors of the vacancy, resulting from their 2% radial relaxation inward.

Large overlaps for cation interstitials between cations (especially Cd between Cd), as well as for hexagonal interstitials, lead to larger relaxations outward for tetrahedral cation interstitials between cations than for cation interstitials in the preferred tetrahedral position (between anions). The nearest neighbors of the Cd interstitial between Cd in CdTe relax outward by about 6%, compared with relaxations of 3%–4% for Cd, Hg, and In interstitials in the preferred tetrahedral position in $Hg_{1-x}Cd_xTe$.[1]

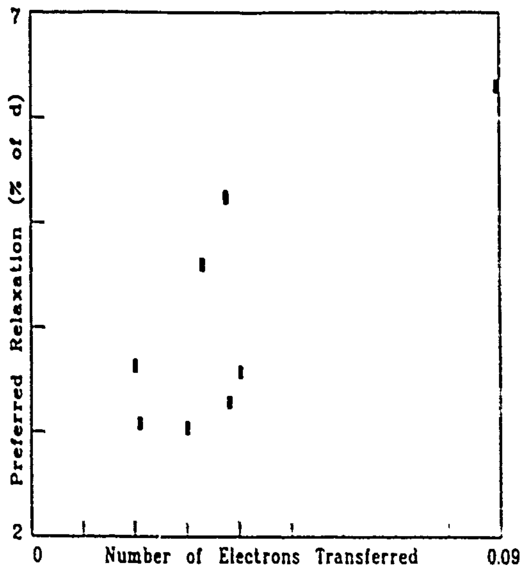

FIG. 1. Plot of predicted minimum energy relaxation versus the number of electrons transferred into the interstitial region upon relaxation.

For anion-like interstitials in the preferred tetrahedral position, most of the electronic charge is transferred to the interstitial itself as the lattice relaxes. During relaxation, less charge is transferred to the anion-like interstitials which have a larger excess negative charge before relaxation. Therefore, we can predict the relative amounts of relaxation outward (3.1%, 4.6%, and 5.2% for As, Sb, and Te) simply by knowing the amount of excess negative charge on these interstitials before relaxation: 0.26, 0.10, and 0.01 e for As, Sb, and Te, respectively, in units of the electronic charge.

V. CONCLUSIONS

Results of self-consistent, tight-binding supercell calculations for the localized electronic levels and lattice relaxations associated with interstitial As, Sb, and Te in CdTe and the Hg vacancy in HgTe have been presented, and trends in the localized levels and relaxations for these defects and for Cd, Hg, and In interstitials, from earlier calculations,[1] have been discussed. The reduction of overlap energies, resulting in a net transfer of electronic charge into the defect region, drives the relaxation for all these defects. Some specific conclusions which may be drawn from these results are given below:

Of interstitials in the preferred tetrahedral position, Te has the largest nearest-neighbor relaxation outward, and is the most likely to be attracted to regions where this extra strain may be accommodated. In Te-rich material, there may also be high concentrations of cation vacancies, which have an inward nearest-neighbor relaxation and may therefore attract Te interstitials. This strain-mediated attraction may promote the creation of Te antisite defects. The large strain energy associated with isolated Te interstitials may also help explain the tendency for excess Te to condense into second-phase Te inclusions.

Large strains are also associated with Cd interstitials at hexagonal sites and tetrahedral sites with cation nearest neighbors. This may explain the apparent unfavorability[2,3] of Cd interstitial diffusion down the open channel between preferred tetrahedral sites, since this path passes through tetrahedral sites with cation nearest neighbors and hexagonal sites.

Defect level energies for anion-like interstitials in their preferred tetrahedral position (between cations) and for cation-like interstitials in their preferred tetrahedral position (between anions) both show a downward trend with decreasing atomic orbital energies on the interstitial.

Vydyanath has suggested that the midgap tunneling centers in Hg-rich HgCdTe may be due to Hg interstitials, based on his experimental work in various overpressures of Hg.[18] Previous calculations using the less accurate small-basis method[19] have shown a deep level of A_1 symmetry in the gap region, due to the Hg interstitial in the preferred tetrahedral position. In this work, we find that the A_1 level which holds the last two electrons for the Hg interstitial in the preferred tetrahedral position appears to be located close to the conduction band edge in Hg-rich HgCdTe. This interstitial therefore remains a candidate for providing tunneling levels in the gap. The 3% outward relaxation of the Te nearest neighbors of this interstitial allows the A_1 level to become more localized on the interstitial itself, and to move slightly lower in the gap.

ACKNOWLEDGMENTS

This work was supported by the Night Vision and Electro-Optics Laboratories and the ARO under ARO Grant Nos. DAAL03-87-K-0061 and No. DAAG29-85-K-0119, and by the Institute for Manufacturing Research.

[1] J. T. Schick and C. G. Morgan-Pond, Semicond. Sci. Technol. (to be published).
[2] M.-F. Sung Tang and D. A. Stevenson, J. Vac. Sci. Technol. A 7, 544 (1989).
[3] C. G. Morgan-Pond, J. T Schick, and S. Goettig, J. Vac. Sci. Technol A 7 354 (1989).
[4] Y. Bar-Yam and J. D. Joannopoulos, Phys. Rev. B **30**, 1844 (1984).
[5] G. A. Baraff and M. Schluter, Phys. Rev. B **30**, 3460 (1984).
[6] D. J. Chadi, in 1988 Proceedings of the World Materials Conference and references therein (to be published).
[7] D. Tománek, C Sun, N. Sharma, and L. Wang, Phys. Rev B **39**, 5361 (1989).
[8] J. T. Schick and C. G. Morgan-Pond, Bull. Am. Phys. Soc. **34**, 456 (1989) (to be published).
[9] J. A. Majewski and P. Vogl, Phys. Rev. B **35**, 9666 (1987).
[10] W A Harrison, *Electronic Structure and the Properties of Solids* (Freeman, San Francisco, 1980).
[11] W. A. Harrison, Phys. Rev. B **31**, 2121 (1985).
[12] M. P. Tosi, Solid State Phys. **16**, 1 (1964).
[13] R. Hoffman, J. Chem. Phys. **39**, 1397 (1963).
[14] E. Clementi and C. Roetti, At. Data Nucl. Tables **14**, 177 (1974).
[15] J. P. Desclaux, At. Data Nucl. Data Tables **26**, 197 (1981).
[16] C. E. Moore, *Atomic Energy Levels* (NIST, Gaithersburg, MD, 1949)
[17] S. Goettig and C G. Morgan-Pond, Mat. Sci. Forum **38–41**, 317 (1989) (to be published).
[18] H. R. Vydyanath (private communication).
[19] S. Goettig and C. G. Morgan-Pond, J. Vac. Sci. Technol. A **6**, 2670 (1988) (to be published).

]

PHYSICAL REVIEW B VOLUME 42, NUMBER 18 15 DECEMBER 1990-II

Formation mechanisms of localized interstitial states in tetrahedrally bonded semiconductors

S. Goettig
Institute of Physics, Warsaw University of Technology, Koszykowa 75, 00-662 Warszawa, Poland

C. G. Morgan-Pond
Department of Physics and Astronomy, Wayne State University, Detroit, Michigan 48202

(Received 11 January 1990)

The processes of formation of the localized defect states due to tetrahedral and hexagonal *sp*-type interstitials in *sp*-bonded materials are considered using a simple, tight-binding-type local-matrix approach. In this method we subsequently account for the interaction of the interstitial with its nearest neighbors, and for the covalent, polar, as well as metallic couplings in the small system of bonds surrounding the defect. The deep and hyperdeep levels, as well as resonances of different symmetries, are discussed and are shown to derive either from the atomic states on the interstitial, or from various host states on the surrounding atoms. The level-formation schemes for the P interstitial in GaP, self-interstitials in Si, and Hg interstitials in CdTe are presented.

I. INTRODUCTION

During the past decade considerable progress in calculations of localized defect states has been made. A variety of approaches based on the Green's-function method, and ranging from simple semiempirical to sophisticated self-consistent local-density formalisms, has been used to improve our knowledge of the basic properties of localized states. However, no simple interpretation of the results obtained follows from the Green's-function method itself. In particular, neither the origins of the complicated spectrum of localized levels and resonances, nor the character of these levels, can be explained by the method. The Green's-function approaches also shed no light on the important role of the local environment of the defect in the process of formation of localized states, giving no transparent picture of the formation of these states from the atomic states on the defect and the surrounding host atoms.

To interpret the Green's-function results, simple, usually defect-molecule-like, local models have been used for substitutional[1] and interstitial[2-4] defects. However, due to their often schematic character, or the simplifying assumptions made, the presently existing interpretations give a limited and often incomplete physical insight into the process of the formation of localized states.

In this paper we give a far more detailed analysis of the formation processes of localized states, focusing on *sp*-type interstitials in tetrahedrally bonded semiconductors. We use the local-matrix approach developed in the preceding paper[5] (to be referred to as I), and apply it to tetrahedral and hexagonal interstitials. As discussed in I, this simple tight-binding-type approach results in a good qualitative and often quantitative agreement with more sophisticated self-consistent Green's-function calculations, and thus may provide us with a fairly realistic picture of the formation processes. The method allows us to consider the formation of the localized states not only in homopolar crystals such as Si,[2-4] but also in materials with strong polar and metallic couplings such as $Hg_{1-x}Cd_xTe$. We interpret both deep and hyperdeep states, as well as hostlike resonances (or levels), often present in the midregion of the valence band of tetrahedrally bonded semiconductors, whose origins have not yet been analyzed. The distributions of charge density associated with the localized states are also directly interpreted in terms of the parent states.

In Sec. II we briefly present the local-matrix method. Then, following closely the course of discussion adopted in paper I, in Sec. III we examine the formation processes for the tetrahedral P interstitial in GaP, for tetrahedral and hexagonal self-interstitials in Si, and finally for Hg tetrahedral and hexagonal interstitials in CdTe.

II. METHOD

Let us briefly summarize the basic assumptions of the local-matrix method,[5] which sets a framework for the present analysis of formation mechanisms. In this method, a local system of bonds surrounding the defect is softly decoupled from the infinite *sp*-bonded host crystal, and described in terms of the local matrix. The soft-decoupling procedure preserves all the covalent (strongest) bonds, while neglecting other, weaker interactions that couple the local system to the rest of the host crystal. In addition to the covalent interaction, we account for the metallic coupling (promotion energy) and polar coupling in the system. The interaction between the interstitial and its nearest neighbors is treated exactly, within the assumed two-center approximation.[6] The interaction between the host atoms is considered within the nearest-neighbor approximation. The values of tight-binding parameters entering the local matrix, as well as the reference position of the valence-band edge, are the same as in the host crystal from which the local system has been decoupled. The position of the top of the valence band is thus given by the sp^3 nearest-neighbor

©1990 The American Physical Society

tight-binding calculation for the perfect host crystal, with the same values of tight-binding parameters as those used in the local matrix.

For the tetrahedral and hexagonal interstitials we consider the local matrix that involves 36 and 40 basis states (s and p orbitals, and/or sp^3 hybrids) located on 15 and 19 atoms, respectively. Namely, we include in the calculation all states on the interstitial and on its nearest neighbors (1NN atoms), and all those hybrids on further neighbors, which are covalently bonded to hybrids on the nearest neighbors (the further-neighbor atoms that have covalent bonds with the 1NN atoms will be called the 2NN atoms; see Fig. 1 in I). The values of the on-site tight-binding matrix elements $E_s^{(\kappa)}$ and $E_p^{(\kappa)}$, where κ denotes the atomic species, are taken[5] from atomic data for the s and p levels, respectively. The off-site tight-binding matrix elements for both host-host and host-defect nearest-neighbor interactions assume the empirical $1/d^2$-scaled values.[7]

At each stage of the formation process we solve[8] the eigenvalue equation for the local matrix considered in I, in which appropriate (for the considered stage) tight-binding interactions are taken into account. We start with the system composed of isolated atoms (i.e., the system with all off-site elements neglected), and subsequently include the interactions between the atoms in order of the increasing importance. To characterize the states of the system at each step of the formation process, along with the energy of each state, we also calculate the corresponding probability of finding the electron on the interstitial site, on all 1NN atoms, and on all 2NN atoms. This probability (or charge) distribution, expressed in percent, is given in parentheses for each energy level shown in the figures discussed in the next section. All parameters used in the present calculation assume the values listed in Sec. V of I.

III. RESULTS

In this section we discuss the formation mechanisms for several tetrahedral and hexagonal interstitials in GaP, Si, and CdTe, following the course of discussion presented in I.

A. The tetrahedral P interstitial in GaP

The localized states obtained in the local-matrix approach for the neutral P interstitial (with P nearest neighbors) at the tetrahedral (T_d symmetry) site in GaP have been discussed in I, giving a good agreement with the results of self-consistent Green's-function calculations.[9] Here we will consider the process of formation of these states, which is presented in Fig. 1, and consists of the following stages.

(i) Panel (a) shows the energy levels $E_s^{(\delta)}$ and $E_p^{(\delta)}$ of the isolated interstitial ($\kappa=\delta$) atom, and the energy level E_1 of the dangling sp^3 hybrids on the 1NN atoms. Here, $E_\kappa=\frac{1}{4}(E_s^{(\kappa)}+3E_p^{(\kappa)})$, with $\kappa=1,2$ for the 1NN and 2NN atoms, respectively. All the interactions between orbitals on different atoms, and the promotion energy on the 1NN atoms, are neglected at this stage. The states of the noninteracting system corresponding to energies $E_s^{(\delta)}$ and $E_p^{(\delta)}$ have all the charge located on the interstitial, and the states with the energy E_1 have all the charge distributed among the 1NN atoms. We observe that the system composed of noninteracting atoms also has states with energy E_2, i.e., the energy of atomic states on the 2NN atoms (we note that according to the soft-decoupling procedure we always neglect[5] the promotion energy on the 2NN atoms). These states, whose charge is distributed entirely among the 2NN atoms, do not participate in the first stage of formation, and will be included later.

(ii) Panel (b) shows the splitting of the levels, which is due to the interaction of the dangling hybrids on each 1NN atom with the interstitial hybrid that points toward this atom. [This interaction is described[10] by the matrix elements $\rho_{s\pm}$ and $\rho_{p\pm}$ given by Eqs. (13) and (14) of I, re-

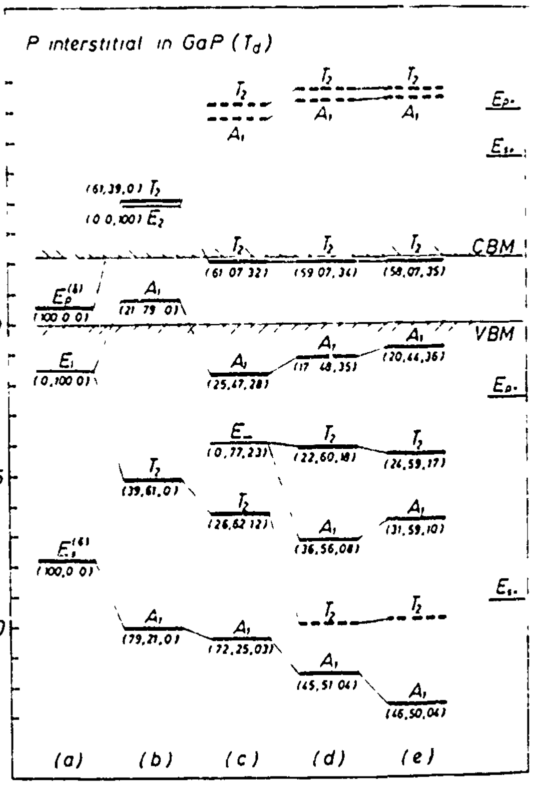

FIG. 1. Formation of the localized states due to the tetrahedral P interstitial (with P nearest neighbors) in GaP. Formation stages: (a) isolated atoms; (b) including the (leading part of the) interaction of the interstitial orbitals with dangling hybrids on the 1NN atoms; (c) including the covalent coupling between hybrids on the 1NN and 2NN atoms; (d) including the promotion energy on the 1NN atoms; (e) including the remaining interactions between the interstitial and the 1NN atoms (see details in text). Notation: localized states, thick solid lines; weakly localized or extended states, dashed lines; parent host states, thin solid lines; (a,b,c), fractional charge (in percent) on the interstitial, on all 1NN atoms, and on all 2NN atoms, respectively. The energies of the system without the interstitial $E_{s\pm}$ and $E_{p\pm}$ (see text) are indicated on the right-hand side of the figure.

spectively.] The rest of the defect-host interactions, less significant for the formation process, will be included later. The levels split into a pair of bondinglike levels of A_1 (s-like) and T_2 (p-like) symmetry located in the valence band, and a pair of A_1 and T_2 antibondinglike levels located above the top of the valence band.

(iii) Panel (c) shows the result of including the covalent coupling β between the host atoms; i.e., the dangling hybrids on the 1NN atoms now form covalent bonds with the hybrids on the 2NN atoms. Due to this interaction, the three lower levels of panel (b) are shifted downward in energy, while the upper T_2 level goes upward, loses a lot of charge on the interstitial site, and becomes a weakly localized level (denoted by a dashed line). A pair of new A_1 and T_2 states is also formed. The formation of these new states may be seen as resulting from the interaction of the already existing states (of A_1 and T_2 symmetry, respectively) with the above-mentioned host states (of the system composed of noninteracting atoms) localized on the 2NN atoms and having the energy E_2. The energy level corresponding to these states is indicated in panel (b) at about +4 eV. Due to this interaction all the previously existing levels are shifted as described above, while the E_2 level splits into a pair of a strongly localized T_2 level and a delocalized A_1 level (denoted by a dashed line). We observe, however, that because the E_2 level and the T_2 level at +4 eV in panel (b) are very close to each other, the resulting localized T_2 state [at about +2 eV in panel (c)] has a strongly mixed character. Hence, its association with the parent level E_2 has, in this case, a rather conventional character, and we may as well consider this T_2 level to be derived from the T_2 level at +4 eV in panel (b).

(iv) Panel (d) shows the result of including the promotion energy Δ_1 on the 1NN atoms, i.e., now the hybrids on the same 1NN atoms can interact with each other; here, $\Delta_1 = -\frac{1}{4}(E_s^{(1)} - E_p^{(1)})$. For the states of A_1 symmetry, the most significant effect due to this interaction is the formation of a third localized state of A_1 symmetry, located below the top of the valence band. The formation of the third localized A_1 level may be viewed as resulting from the interaction of the two[11] already existing A_1 localized states with the bonding A_1 symmetry host state of the system formed due to the covalent (and also polar) interaction between the 1NN and 2NN atoms (namely, the A_1 state of the system without a defect, with the energy given by Eq. (5) of I, taken for the minus sign, and with $\Delta_1 = 0$, i.e., with the energy $E_- = \frac{1}{2}\{E_1 + E_2 - [(E_1 - E_2)^2 + 4\beta^2]^{1/2}\}$). This host state, with the energy E_-, is located between the two A_1 localized states of panel (c), close to −4 eV. The interaction between these three states pushes the upper A_1 localized level towards the top of the valence band and pushes down the lower A_1 level out of the valence band, while the host state is pulled down into the valence band, assumes the localized character, and forms the third A_1 localized level. A similar process occurs for the T_2 states. Again, we have two T_2 localized states interacting with the bonding T_2 symmetry host states formed due to the covalent interaction between the 1NN and 2NN atoms [i.e., the T_2 states of the system without a defect, with the energy given by Eq. (6) of I, taken for the minus sign, and with $\Delta_1 = 0$]. The host level (with the same energy E_- as in the case of the A_1 host state, considered above) is again located between the two localized T_2 levels of panel (c). Due to the interaction of these three states, the upper T_2 localized level remains almost unaffected, the host level is slightly pushed down in energy, assumes a localized character, and forms the second T_2 level [at around −4 eV in panel (d)], while the lower T_2 level is strongly pushed down in energy, loses a lot of charge on the interstitial site, and becomes a weakly localized level (denoted by a dashed line). We note that inclusion of the promotion energy on the 1NN atoms leads also to the interaction with the antibonding A_1 and T_2 symmetry host states of the system with the energy E_+, formed due to the covalent interaction between the 1NN and 2NN atoms (namely, the A_1 and T_2 states of the system without a defect, with energies given by Eqs. (5) and (6) of I, respectively, taken for the plus sign, and with $\Delta_1 = 0$, i.e., with the energy $E_+ = \frac{1}{2}\{E_1 + E_2 + [(E_1 - E_2)^2 + 4\beta^2]^{1/2}\}$), and located at around +6 eV. However, this coupling results in states that are not localized, and thus, for the sake of clarity, not displayed in Fig. 1.

(v) Panel (e) shows the result of including the remaining interactions between the interstitial and the 1NN atoms [i.e., those described by the matrix elements $\nu_\pm$, $\eta_\pm$, and $\mu_\pm$ given by Eqs. (15)–(17) of I]. The main effect due to these interactions is the further reduction of the $A_1 - T_2$ splitting of the levels in the fundamental gap region, and further lowering of the hyperdeep A_1 level. On the right-hand side of Fig. 1 we also show, for comparison, the energies $E_{s\pm}$ and $E_{p\pm}$ [given by Eqs. (5) and (6) of I] of the system without the interstitial (but with all other interactions included). To each of these levels there corresponds one state of A_1 symmetry and three states of T_2 symmetry.

The above analysis indicates that two of the obtained localized states may be seen as originating from the atomic states of the interstitial; namely, the T_2 deep state in the gap derives from the p atomic state of the interstitial (see the discussion above) and the lowest A_1 hyperdeep states derives from the s atomic state of the interstitial. The large amount of charge on the interstitial found for these states, as well as a strong variation of their energies with changes in the atomic energies on the interstitial, are consistent with this picture. Therefore, these two states may be called defectlike. We note that both of these states are substantially mixed with the host states; for example, the deep T_2 state is strongly mixed with the E_2 state localized on the 2NN atoms, and because of that it has most of the remaining charge localized on the 2NN atoms.

The remaining three localized states have a hostlike character: the gap-region A_1 localized state derives from the host states of the 1NN atoms, while a pair of A_1 and T_2 mid-valence-band states derive from the host states formed from covalent bonds between the 1NN and 2NN atoms. All of these three states have smaller charges on the interstitial and weaker variations of their energies

)-4

with the change of atomic energies on the interstitial. These variations of energies are especially weak for the mid-valence-band states, which reflects their strongly hostlike character, and are consistent with the behavior observed for such states in the self-consistent Green's-function calculations.

B. Tetrahedral self-interstitials in Si

We shall now consider the formation of localized levels due to the neutral tetrahedral self-interstitial in Si. The comparison of the results of the present approach with the self-consistent Green's-function calculations[12] have been discussed in I. Since many features of the formation process, presented in Fig. 2, are similar to the previously considered case of the P interstitial in GaP, in our discussion below we will mainly focus on differences between these two cases.

As for the P interstitial in GaP, the E_1 level corresponding to host states located on the 1NN atoms lies between the $E_s^{(\delta)}$ and $E_p^{(\delta)}$ energies on the interstitial, and the levels resulting due to the leading part of the interaction between the interstitial and the 1NN atoms, shown in panel (b), are qualitatively similar to those obtained for P in GaP. The difference occurs when the covalent coupling β between the 1NN and 2NN atoms is included. Now the energy E_2 $(E_2=E_1)$ of the host states located on the 2NN atoms lies between the two pairs of A_1 and T_2 levels of panel (b). Due to this, both the A_1 and T_2 states formed in the gap region [panel (c)] derive form the host E_2 states, and have most of the charge located on the 2NN atoms. Now, unlike for P in GaP, also the hyperhigh T_2 level (resonance) in the conduction band is localized. The inclusion of the promotion energy on the 1NN atoms [panel (d)] results, similarly as for P in GaP, in the formation of a pair of new A_1 and T_2 states located in the middle of the valence band. They derive from the E_- $(E_\pm=E_1\pm|\beta|)$ bonding A_1 and T_2 symmetry host states of the system, respectively (see Sec. III A for details). We note that the E_- states now contain more charge on the 2NN atoms than in the case of P in GaP, and due to that the localization of the resulting A_1 state (at about -5 eV) is weaker than for the comparable state for P in GaP, while the localization of the T_2 state (at about -4.5 eV) becomes very weak, and thus this level is denoted by a dashed line. As in the case of the P interstitial in GaP, the antibonding host states with the energy E_+ do not give rise to any localized states. The inclusion of the remaining direct interactions between the interstitial and the 1NN atoms [panel (e)] leads to the same effects as for P in GaP. We observe that, similar to that case, these interactions do not practically affect the positions of the levels of T_2 symmetry. The distribution of the total charge between the interstitial, all the 1NN atoms, and all the 2NN atoms is also weakly affected by these interactions, though the wave function itself can experience significant changes (up to 100%) on single sites. It is also worthwhile to note that although the A_1 state located at about -2 eV in panel (e) has most of its charge located on the 2NN atoms, it is still a well-localized state. It has 29% of charge located on the interstitial, about 3% on each 1NN atom, about 7% on each 2NN atom from the second shell, and about 5% on each 2NN atom from the fourth shell. Thus, the charge on the interstitial site is significantly larger than on any other single site, which, according to our criteria discussed in I, classifies this state as localized.

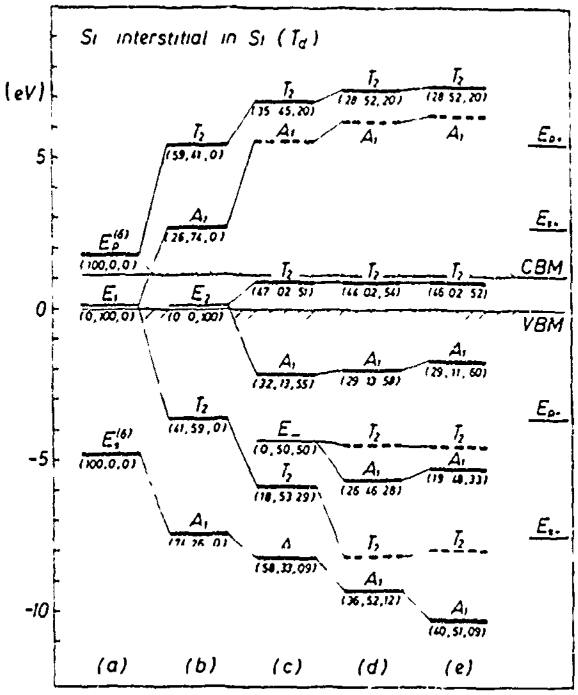

FIG. 2. Formation of the localized states due to the tetrahedral self-interstitial in Si. Formation stages and notation as in Fig. 1.

The above analysis of the level formation for the tetrahedral self-interstitial in Si shows that, as in the case of P in GaP, the hyperdeep A_1 state has a defectlike character, deriving from the s atomic state on the interstitial. We note the strong mixing of this state with the E_1 and E_- host states. The T_2 gap state derives from the host states localized on the 2NN atoms. It has, however, a very strong component coming from the $E_p^{(\delta)}$ state on the interstitial. This T_2 state also has a large charge on the interstitial, and the strongest variation of its energy with changes in the $E_p^{(\delta)}$ energy on the interstitial. Thus, we would characterize this level as predominantly defectlike. The two upper A_1 localized states in the valence band, as well as a weakly localized T_2 state at about -4.5 eV, are hostlike. They have smaller charges on the interstitial, and weaker variations of the energies with changes of atomic energies on the interstitial.

C. The hexagonal self-interstitial in Si

The process of formation of the localized states due to the neutral hexagonal self-interstitial in Si is shown in Fig. 3. The formation stages are similar, but not identical to those discussed above for the tetrahedral interstitial, and are as follows.

ı–5

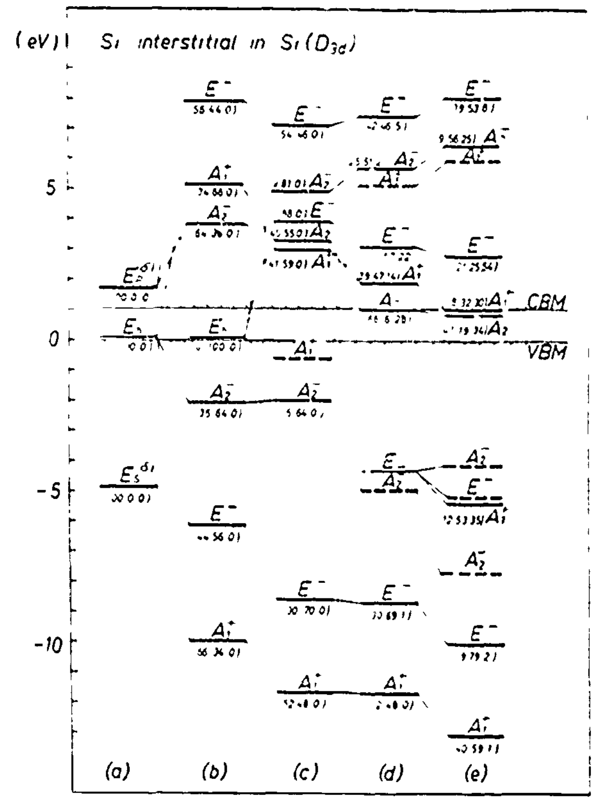

FIG 3 Formation of the localized states due to the hexagonal self-interstitial in Si. Formation stages: (a) isolated atoms; (b) including the interaction of the interstitial orbitals with dangling hybrids on the 1NN atoms; (c) including the covalent coupling between hybrids on the 1NN atoms in the hexagonal ring; (d) including the covalent coupling between hybrids on the 1NN and 2NN atoms; (e) including the promotion energy on the 1NN atoms. Notation as in Fig. 1.

(i) Panel (a) show the energy levels $E_s^{(\delta)}$ and $E_p^{(\delta)}$ of the isolated interstitial atom, and the energy level E_h of the dangling sp^3 hybrids on the 1NN atoms. Note that in the homopolar material the hybrid energies on all 1NN atoms are the same: $E_h = E_1 = E_2$. All interactions between orbitals on different atoms, and the promotion energy on the 1NN atoms, are neglected at this stage.

(ii) Panel (b) shows the splitting of the levels due to the interactions of s and p orbitals on the interstitial with the dangling hybrids on the 1NN atoms. Due to the lower (D_{3d}) symmetry of the hexagonal site, the meaningful decomposition of the interstitial–host-atoms interaction into more and less significant parts, utilized in the tetrahedral case, cannot be made. Therefore, the full interaction between the interstitial and the 1NN atoms is included here. The E_h level splits into a set of bondinglike levels of A_1^+ (s-like), E^- (p_x,p_y-like), and A_2^- (p_z-like) symmetry located below the top of the valence band, and a similar set of antibondinglike levels located in the conduction band. The p_x and p_y orbitals on the interstitial, lying in the plane of the puckered hexagon, interact with the 1NN atoms more strongly than the p_z orbitals, which leads to a larger splitting between the E^- bonding and antibonding states than seen for the A_2^- states.

(iii) Panel (c) shows the effect of including the covalent coupling between the 1NN atoms that form the hexagonal ring around the interstitial: now two hybrids on each 1NN atom are involved in covalent bonds in the ring, while two remaining hybrids on each 1NN atom are still dangling (compare to Fig. 1 in I). The coupling strongly shifts down the energies of A_1^+ and E^- hyperdeep as well as hyperhigh states. Some new localized states are also formed. They arise from the E_h host states located on the 1NN atoms. (The degeneracy of the E_h level was not completely removed by the host-defect interactions considered in the previous stage, and now it splits again due to the covalent interactions in the ring.[13]) The E_h level splits into A_2^- and E^- localized levels placed in the conduction band, and a delocalized A_1^+ state (mostly composed of the dangling hybrids on the 1NN atoms) placed just below the top of the valence band. We observe a strong shift in the characters of the two A_2^- levels placed in the conduction band. The upper one (at +5 eV) is strongly localized on the 1NN atoms, and the lower one (at +3.5 eV) has a significant amount of charge on the interstitial. However, the characters of the levels they derive from are reversed, namely the upper A_2^- state in panel (b) is strongly localized on the interstitial, while the lower one is the E_h host state localized on the 1NN atoms. Since the shift in the character of the states is so drastic here, we have chosen to connect (by dashed lines) the A_2^- levels of an alike character, rather than to follow the movement of the levels when β interactions in the ring were slowly increased from zero (in the latter case, clearly, the levels would not cross). In future cases, when there is such a clear shift in the character of the states that we must show the two states of the same symmetry crossing in order to follow the character of the states, we will use similar dashed lines.

(iv) Panel (d) shows the effect of including the remaining covalent interactions between the host atoms, i.e., the covalent coupling between the 1NN and 2NN atoms. [Note that panel (d) for the hexagonal case is equivalent to panel (c) for the tetrahedral case.] The hyperdeep A_1^+ and E^- states are almost unaffected by these interactions, since in stage (c) these states have almost all of the charge located on the interstitial or engaged in the ring bonds. In contrast, the lowest A_2^- state at −2 eV in panel (c) consists mostly of a bondinglike combination of dangling hybrids on the 1NN atoms and the p_z orbital on the interstitial. Since this coupling is considerably weaker than the covalent bonds between the 1NN and 2NN atoms, the considered A_2^- state loses a lot of charge on the interstitial when these bonds are formed, and becomes delocalized. This charge on the interstitial site may be seen as shifted to the higher A_2^- state found at the bottom of the conduction band in panel (d). For the A_1^+ levels in the gap region we find again a strong shift in the characters, which is why these levels were connected by the dashed lines.

(v) Panel (e) shows the effect of including the promotion energy on the 1NN atoms. As in the case of the tetrahedral self-interstitial, this interaction lowers the energy of the hyperdeep states and increases the energy of

D-6

the hyperhigh states. Also, similar to the tetrahedral case, it leads to the formation of a new A_1^+ localized hostlike state, which derives from the bonding E_- ($E_\pm = E_1 \pm |\beta|$) host states, formed due to the covalent interaction between the 1NN and 2NN atoms in the hexagonal system with no interstitial.

When the promotion energy on the 1NN atoms is included, some states derive also from the antibonding host states with the energy E_+ (located at about +4.5 eV). In the case of the tetrahedral self-interstitial the resulting A_1 state is extended, while the T_2 state has a clear surface character. However, for the hexagonal self-interstitial, the E_+ host states give rise to the A_2^- state of a rather weak surface character, but with a considerable amount of charge (about 20%) on the interstitial, and the energy strongly shifted downward (to about +2.5 eV). This could suggest that we have obtained a second localized A_2^- state in the gap region. However, obviously, the considered A_2^- hexagonal state splits (when going from the T_d to the D_{3d} site) from the above-mentioned T_2 surface state. This strongly indicates that the considered A_2 state is a spurious quasilocalized state whose properties derive from the small size and particular form of the hexagonal system, i.e., such a state should not be observed as localized in the bulk crystal. This conclusion is supported by other calculations,[14] which also find a single A_2^- state in the gap region. The spurious A_2^- state formed just above the localized A_2^- level may be seen as being responsible for the incorrect ordering of levels seen for the hexagonal Si self-interstitial in the gap region: the A_1^+ level should lie below[14,15] the A_2^- and E^- levels, as it does for the other three groups of states in panel (e). Namely, the spurious A_2^- state, which acquires a lot of charge on the defect site from the localized A_2^- gap state, repels it further down in energy, which is why the A_2^- localized state stays below[16] the A_1^+ gap state.

Comparing the final structures of the levels obtained for the tetrahedral and the hexagonal self-interstitials, we find that (as it should be) to each tetrahedral A_1 level there corresponds one hexagonal A_1^+ level, while each tetrahedral T_2 level splits into a pair of A_2^- and E^- hexagonal levels, with the characters of the corresponding levels basically preserved during the transition from the T_d to the D_{3d} site. We observe that when this transition occurs, the very weakly localized T_2 hyperdeep level gives rise to the localized E_- hyperdeep level, seen also in other calculations.[14,15]

D. Tetrahedral and hexagonal Hg interstitials in CdTe

In paper I, we calculated the localized states due to indium and self-interstitials in $Hg_{1-x}Cd_xTe$. Here, as an example, we have chosen to discuss the formation of the localized states due to the Hg interstitial in pure CdTe. In the tetrahedral case, we will consider only the preferred position of the Hg interstitial, i.e., that with anion nearest neighbors;[17] this interstitial may be responsible for providing the midgap tunneling levels in the mercury-rich compound.[5] We note that since In, and also Cd, have values of the s and p atomic energies close to those of Hg, the results shown below are also typical for these interstitials.

Let us start with the formation process due to the tetrahedral Hg interstitial (with Te nearest neighbors) shown in Fig. 4. We first observe that, unlike in the previously considered case of P in GaP (i.e., also an interstitial with anion nearest neighbors), or in the case of the self-interstitial in Si, now both $E_s^{(\delta)}$ and $E_p^{(\delta)}$ energies on the defect lie above the E_1 energy on the 1NN atoms [panel (a)]. This change of the ordering of the parent levels on isolated atoms has profound implications on the character of some finally formed localized states. In particular, the finally formed A_1 gap state [at about +1 eV in panel (e)] now has a defectlike character, deriving directly from the atomic s state on the interstitial and having half of its charge located on the interstitial. Furthermore, the hyperdeep A_1 state is now delocalized, while in the previously considered cases the comparable A_1 hyperdeep states had a strongly localized defectlike character. The mid-valence-band A_1 resonance is, as in the previously considered formation processes, of predominantly hostlike character, with most of its charge located on the 1NN atoms. Among the states of T_2 symmetry the lowest localized one is placed in the conduction band at about +4 eV. This predominantly hostlike state originates from atomic states on the 2NN atoms, and has most of its charge located on the 2NN atoms from the second shell, with only minute charges on the 1NN atoms and on the 2NN atoms from the fourth shell. We may observe a similarity of the character of this T_2 state to the T_2 gap states found previously for P in GaP and for the self-interstitial in Si. The hyperhigh T_2 state now has

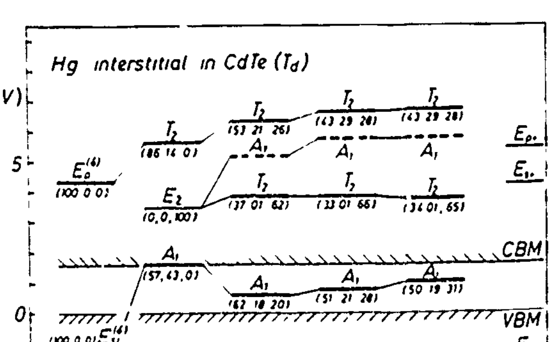

FIG. 4. Formation of the localized states due to the tetrahedral Hg interstitial (with Te nearest neighbors) in CdTe. Formation stages and notation as in Fig. 1.

a defectlike character, deriving directly from the p atomic state on the interstitial.

The formation of the localized levels due to the hexagonal Hg interstitial in CdTe is shown in Fig. 5. For the considered heteropolar material the formation scheme differs from that in a homopolar one (such as Si), since now the interstitial has both anion and cation nearest neighbors (which lowers the symmetry of the defect site to C_{3v}). Thus, in panel (a), apart from s and p atomic energies on the Hg interstitial, we now have both E_1 and E_2 energies of the dangling hybrids on both kinds of the 1NN atoms (i.e., on Te and Cd atoms, respectively). When the orbitals on the interstitial are allowed to interact with these 1NN hybrids, in panel (b), each of the E_1 and E_2 levels splits into a level of E symmetry (p_x,p_y-like) and two levels of A_1 symmetry (s,p_z-like); the upper level of A_1 symmetry arising from the E_1 level is delocalized and not shown in panel (b). The two lowest A_1 levels in panel (b) are primarily of s character on the interstitial, and remain so throughout the entire process of formation. The lower A_1 level arising from the E_2 level is primarily of z character on the interstitial, while the upper A_1 level connected by a dashed line to the E_2 level, from which it derives, is of mixed s and z character on the interstitial. The upper A_1 level connected by a dashed line to the p level on the interstitial has a strong z character on the interstitial. As more interactions are added, the levels shift, but there are few additional levels or splittings. The additional levels arising in panel (c), from the inclusion of the covalent interaction between the 1NN atoms, are hardly localized at all, and are not shown. As in the case of the self-interstitial in Si, when the covalent interactions between the 1NN and 2NN atoms are added in panel (d), the strongly localized level of z character, arising from the p orbitals on the interstitial, is shifted downward, while the less localized A_1 level arising from the E_2 level is shifted upward. Following the character of these strongly mixing states, the crossing of these two levels is shown by dashed lines between panels (c) and (d). In panel (d), all of the s character on the interstitial in the upper three A_1 states has shifted into the middle one of these three states, which becomes progressively more delocalized in panels (d) and (e). As in the case of the hexagonal self-interstitial in Si, the addition of the promotion energy on the 1NN atoms gives rise to few more states. These includes the localized A_1 state [at about −5 eV in panel (e)], which derives from the bonding E_- host states formed due to the covalent (and polar) interaction between the host atoms. The antibonding E_+ host states give rise to the surfacelike state of A_1 symmetry (compare to Sec. III C), which falls between the strongly localized defect states of A_1 symmetry in the gap region in panel (e). However, now the charge on the defect site for this state is smaller than for the Si self-interstitial, and its influence on the localized A_1 states in the gap region is weaker; in particular, the defect A_1 state of strong z character on the interstitial remains above the defect state of strong s character.

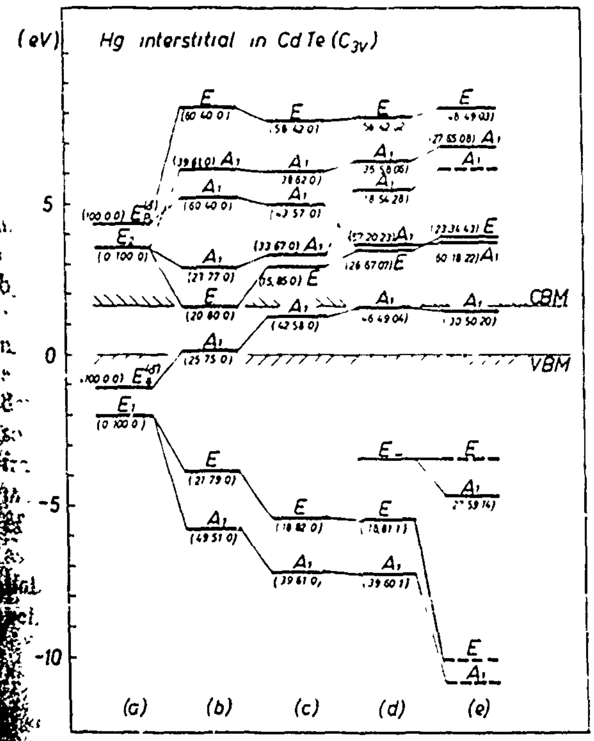

FIG. 5 Formation of the localized states due to the hexagonal Hg interstitial in CdTe Formation stages and notation as in Fig. 3.

IV. CONCLUSIONS

We have presented a simple picture of the formation processes of interstitial defect states, which allows us to interpret the complicated structure of the localized levels in terms of a few basic interactions in the system consisting of the interstitial and a small number of atoms from its close vicinity. We have shown that the localized states can derive either from atomic states on the interstitial, or from host states on the neighboring atoms. These host states can be either simple sp^3-hybrid states on the isolated host atoms, or the states that are formed due to the covalent interactions between the host atoms. The latter states, in particular, give rise to the mid-valence-band resonances of a strong hostlike character. We found that, while the structure of the finally formed levels is basically similar for all the (respective tetrahedral and hexagonal) interstitials considered, the characters of some of the states and the degree of their localization depend in an essential way on the ordering (and values) of the atomic energies on the isolated interstitial and host atoms. For example, the A_1 symmetry tetrahedral gap-region state has a hostlike character for interstitials with relatively large values of s atomic energy (as for P in GaP or the self-interstitial in Si), while it may be strongly defectlike for interstitials with relatively low values of the s atomic energy (as for Hg in CdTe).

We believe that the results presented allow for a fuller understanding of the origins and the nature of the localized defect states. This increased understanding may also be of importance in technological applications involving defects.

ACKNOWLEDGMENTS

One of us (S.G.) acknowledges the hospitality of the International Center for Theoretical Physics in Trieste during the final stages of this work. This work was supported in part by NVEOD and the ARO, under ARO Contracts No. DAAL03-87-K-0061 and No. DAAG29-85-K-0119, and by the Institute for Manufacturing Research.

---

[1] See, e.g., M. Scheffler, J. Bernholc, N. O. Lipari, and S. T. Pantelides, Phys. Rev. B **29**, 3269 (1984).

[2] M. Lanoo and M. Schluter, Phys. Rev. B **31**, 5468 (1985).

[3] O. F. Sankey and J. D. Dow, Phys. Rev. B **27**, 7641 (1983).

[4] P. Boguslawski, G. Papp, and A. Baldereschi, Solid State Commun. **52**, 155 (1984).

[5] S. Goettig and C. G. Morgan-Pond, preceding paper, Phys. Rev. B **42**, 11 730 (1990).

[6] J. C. Slater and G. F. Koster, Phys. Rev. **94**, 1498 (1954).

[7] W. A. Harrison, Phys. Rev. B **27**, 3592 (1983).

[8] For the tetrahedral interstitial we use Eqs. (12), (18), and (21) of I, while for the hexagonal interstitial the local matrix is diagonalized numerically.

[9] M. Scheffler, in *Festkörperprobleme (Advances in Solid State Physics)*, edited by P. Grosse (Pergamon, Braunschweig, 1982), Vol. XXII, p. 115.

[10] In fact, at the present stage of formation this interaction is, as it follows from Eq. (12) of I with the use of Eqs. (5), (6), and (9), completely described by a single parameter $\beta^{(1)}=\frac{1}{2}(\beta_s^2+3\beta_p^2)^{1/2}$. Here, β_s and β_p are defined by the equations $\beta_s C_{s\pm}=\rho_{s\pm}$ and $\beta_p C_{p\pm}=\rho_{p\pm}$ [see Eqs. (13) and (14) of I]. The energies of the two A_1 and two T_2 levels shown in panel (b) of Fig. 1 are given by Eqs. (5) and (6) of I, respectively, with $\beta^{(1)}$ replacing β, E_6 replacing E_1, Δ_6 replacing Δ_1, and E_1 replacing E_2 in these equations.

[11] Of course, the interaction occurs with all states of a given symmetry that are already formed, i.e., also with weakly localized or extended states in the conduction band. However, the influence of these states on the process of formation of localized states is not essential and may be neglected for the purpose of the present analysis.

[12] J. P. Vigneron, M. Scheffler, and S. T. Pantelides, Physica B+C **117**, 137 (1983).

[13] Comparing the parent levels E_h for the hexagonal case with those considered for the tetrahedral one, we have to note that when the interstitial moves from the T_d to the D_{3d} site, some of the 2NN atoms of the tetrahedral interstitial become the 1NN atoms of the hexagonal interstitial.

[14] G. A. Baraff and M. Schluter, Phys. Rev. B **30**, 3460 (1984).

[15] Y. Bar-Yam and J. D. Joannopoulos, Phys. Rev. B **30**, 1844 (1984).

[16] We observe that, unlike for the Al hexagonal interstitial in Si or the Hg hexagonal interstitial in CdTe, for which we obtain the correct ordering of the finally formed gap levels [see Ref. 5 and Sec. III D, respectively], for the self-interstitial in Si the "incorrect" ordering is already present at the stage of the formation process shown in Fig. 3(d). [For the Al interstitial the $E_p^{(6)}$ energy is about 2 eV larger than for the Si interstitial, which strongly pulls up the A_2^- level in Fig. 3(d), into the position between the A_1^+ and E^- levels.] Therefore, for the Si self-interstitial this incorrect ordering has to be *reversed* by adding further interactions. The inclusion of the promotion energy in Fig. 3(e) turns out to be insufficient for this aim, apparently due to the presence of the spurious A_2^- state, and only the account for interactions with further shells of atoms may result in the correct ordering of the gap states. (When these interactions are included, the spurious state gradually merges with the extended states.)

[17] C. G. Morgan-Pond, S. Goettig, and J. T. Shick, J. Vac. Sci. Technol. A **7**, 354 (1989).

PRESENT STATUS AND FUTURE OF THEORETICAL WORK ON POINT DEFECTS AND DIFFUSION IN SEMICONDUCTORS

C. G. Morgan-Pond
Department of Physics and Astronomy, Wayne State University
Detroit, MI 48202 USA

A brief description of the theoretical methods commonly used to investigate point defects and diffusion is given. The current status of theoretical understanding of hydrogen diffusion in silicon, self-diffusion in silicon, and Hg and Cd diffusion in HgCdTe is described, as examples of systems where a basically coherent picture has been achieved, where the many theoretical contributions have not succeeded in resolving a fundamental controversy, and where theoretical work is only in its initial stages. Several exciting new directions which promise expanded theoretical capabilities in the future are indicated.

I. INTRODUCTION

Well-designed experiments and theoretical calculations can provide complementary contributions toward the ultimate goal of complete understanding of point defects and their role in diffusion. Although in some cases, present theoretical methods are not sufficiently accurate to predict which of several competing diffusion mechanisms should dominate, they still offer considerable guidance in the search for a correct description of the microscopic atomic motion during diffusion.

Recent development and refinement of methods involving the local density approximation (LDA)[1-3] to the density-functional theory for the exchange and correlation energy have made possible calculation of the total energies of the more symmetric configurations of a number of point defects with greater quantitative accuracy than the simpler methods which had previously been the most frequently used. However, the amount of computer time required by the new LDA-based methods can severely restrict investigation of systems where the optimal defect configurations involve many degrees of freedom for lattice relaxation, or where many different defect configurations must be considered. For similar reasons, LDA-based molecular dynamics calculations,[4] which allow both defect motion and simultaneous lattice relaxation, are restricted to simulations of high temperature behavior. Fortunately, theoretical developments already in progress promise improved accuracy for the simpler calculations which allow consideration of a wider range of defect configurations, and may permit the use of molecular dynamics methods for temperatures which are currently inaccessible,[5-8] as well as improved accuracy for the more elaborate and computationally demanding calculations.[9-16]

In Section II, the major theoretical techniques which have been used to study point defects and defect-related diffusion: tight-binding, Hartree-Fock-based, and LDA-based pseudopotential and self-consistent Green's function, are reviewed. As an example of successful theoretical characterization, the general picture of the isolated hydrogen interstitial and hydrogen diffusion in silicon, which has now been obtained using a variety of theoretical approaches, is discussed in Section III. Silicon self-diffusion is discussed in Section IV, as an example of a system where present limitations preclude a definitive theoretical determination of the point defect species which dominates diffusion at high temperature. Section V deals with other diffusing species and other materials, for which fewer calculations have been done and many questions remain, including as an example the current status of theoretical contributions to the understanding of Cd and Hg diffusion in HgCdTe. Section VI summarizes what we have learned from theoretical calculations about point defects and diffusion, and indicates some potentially important new directions for the development of more convenient and powerful theoretical tools.

II. THEORETICAL METHODS

In the simplest picture of thermally activated diffusion, mediated by a single point defect and occurring via a single process, the dependence of the diffusion rate on the temperature T is given by

$$\text{diffusion rate} = Ce^{-H/k_BT},$$

where the total enthalpy of the process contains a contribution due to formation of the defect, and a contribution due to its migration:

$$H = H_{\text{formation}} + H_{\text{migration}}.$$

Most of the theoretical work to date has consisted of calculations of total energies for various point defect configurations, or total energy surfaces as a function of atomic position. Such work gives estimates of the formation and migration contributions to the diffusion barrier H, but it cannot give absolute diffusion rates, as it does not consider the entropies of defect formation and migration, which enter the prefactor C. A powerful but expensive alternative approach, the molecular dynamics method recently developed by Car and Parrinello,[4] allows simulation of absolute diffusion rates.

The basic choices which must be made in all of these calculations are (1) what Hamiltonian to use to describe the electron-electron interactions and the energy of the system, and (2) what geometry to use for the crystal, in order to best approximate the behavior of an infinite crystal containing a single, isolated defect.

Empirical tight-binding Hamiltonians were originally proposed only as a useful tool for interpolating band structures. However, the simplicity of tight-binding calculations, and their ability to yield both electronic and structural energies simultaneously, have led to the widespread use of such methods to predict semiquantitatively the electronic and structural properties of bulk materials, surfaces, and point defects, and to obtain qualitative understanding and physical insight. Since tight-binding calculations are less time consuming than first principles Hartree-Fock or LDA-based pseudopotential or self-consistent Green's function calculations, they are especially well suited for investigating systems involving many degrees of freedom, large unit cells, or complicated, non-periodic arrangements of atoms. Recent work on surface reconstruction,[17-22] lattice relaxation around tetrahedral and hexagonal interstitials,[23-25] and the stable configuration of small silicon clusters[26-28] has shown that an empirical tight-binding description of the total energy can be used reliably to predict relaxation for systems close to ideal coordination.

However, in order to compare the total energies of point defect configurations with widely differing atomic coordination, as may occur when atoms diffuse through the crystal, it is necessary to use first-principles-based expressions for the total energy and interactions, which vary as a continuous function of interatomic distance. Recently, it has been shown that various approximations can transform a first-principles density-functional[5,7] or muffin-tin (MT)[29] calculation into the tight-binding form, and a tight-binding approximation to the LDA pseudopotential method, valid for systems with little or no charge transfer, has been successfully implemented for bulk phases and small homopolar molecules.[8] Further development and testing of these first-principles tight-binding methods for the substantially distorted defect configurations, perhaps involving significant charge transfer, which may occur during diffusion, holds the promise of simpler and more rapid calculations of diffusion barriers, and perhaps simulation of absolute diffusion rates, without an unacceptably large sacrifice of accuracy.

In contrast to tight-binding methods, which were originally used with empirically fit parameters, Hartree-Fock methods were developed to include electron-electron exchange as well as direct Coulomb interactions in first principles calculations, with no adjustable parameters. While accurate, particularly if expanded and spin-polarized basis sets are used and corrections for electron-electron correlation are included, *ab initio* Hartree-Fock methods are computationally demanding, and are therefore restricted to atomic, molecular, and small cluster calculations. Use of larger basis sets and correlation corrections increases the computation time substantially. In order to reduce computer costs and make these first principles calculations feasible for larger systems, certain small, four-center integrals may be neglected, resulting in the partial retention of diatomic differential overlap (PRDDO) method.[30-31] *Ab initio* Hartree-Fock and PRDDO calculations using minimal basis sets usually result in overestimates of potential barriers.[32]

In addition to the approximate PRDDO method, Hartree-Fock-based semiempirical methods, such as CNDO (complete neglect of differential overlap),[33] MNDO (modified neglect of diatomic overlap),[34-35] and MINDO (modified intermediate neglect of differential overlap),[36] have been developed for studies involving many calculations, where *ab initio* Hartree-Fock methods would be prohibitively expensive. These methods use parameters fit to experimental data such as atomic ionization potentials, molecular heats of formation, and equilibrium bond lengths in molecules or crystals. Since single-particle energy differences and corresponding total energy differences obtained from semiempirical Hartree-Fock-based cluster calculations can differ substantially, transition energies cannot be gotten simply from the single-particle electron energies in these calculations, as they can in local-density calculations such as the scattered-wave $X\alpha$ (SW-$X\alpha$)[37] method. However, when the parameters are fit to structural data for systems with similar bonding and atomic coordination, these techniques can provide a good description of structural properties and total energy changes as a function of atomic displacement.

The two main LDA-based approaches which have been used to study total energies and diffusion are the self-consistent Green's function[39-40] and a priori pseudopotential[41-43] methods. Local-density methods correctly describe bulk structural properties to within a few per cent of experiment, but they give poor excitation energies: for many semiconductors, the predicted band gap is half the experimental band gap or less. For this reason, the positions of electronic defect levels derived from the conduction band are not accurately given, and total energies of defects with some of these states occupied are also less accurately given than bulk total energies. Much work has been done on correcting the band gap problem in bulk calculations,[10-16] but these corrections have not yet been worked out for systems including defects. The LDA gap has usually been corrected in calculations involving point defects by the rather crude procedure of rigidly shifting the conduction band and conduction-band-derived states upward to coincide with the experimental gap. Estimated error bars for LDA-based calculations are about 1 eV for defect formation energies, and 0.5 eV for migration barriers.[44]

The reliability of any calculation of point defect total energies depends on the geometry of the model system, as well as on the Hamiltonian used. In Green's function methods, the distorted defect region is embedded in a host crystal described by the perfect crystal Green's function. Although self-consistent LDA

Green's function calculations have been carried out for several systems (e.g. References 45 and 46), these methods are computationally complex and very expensive, particularly if the defect region (i. e. the region which is substantially distorted and must be treated exactly) contains more than a few atoms. In addition, the role of the local environment in determining the properties of the defect remains obscure, and often much simpler models must be used to provide a physical interpretation for the results of these calculations.

The less rigorous but more physically transparent approach of the cluster methods is to simulate the infinite crystal by surrounding the defect with a finite number of atoms. The use of small clusters (less than ~100 atoms) rests on the idea that defect properties are most affected by the local environment of the defect. In cluster calculations, the interactions of the finite number of atoms surrounding the defect are treated exactly. Rather than being attached to the rest of the infinite crystal, the clusters are terminated at a certain distance from the defect, often by saturating the dangling bonds at the surface with hydrogen atoms. If the cluster is too small, interactions of the defect with surface states may alter the calculated properties. Particularly when the polarity of the host-saturator bond differs from the polarity of the bulk host bonds so that the charge transfer at the surface is not typical of the charge transfer in the bulk, calculated defect properties may be very sensitive to the host-saturator bond length used, so that to obtain reliable results, care must be taken to terminate the cluster correctly.[47]

In a supercell calculation, the cluster containing the defect is not terminated, but repeated periodically in space to form an infinite crystal. If the repeated cluster is too small, interactions between the point defects may produce a dispersion of the localized defect levels, and lead to calculated total energies which are not the total energies of isolated point defects. Therefore, as for finite cluster calculations, supercell calculations must be tested for convergence as a function of cluster size. In spite of these potential pitfalls, because of their greater physical transparency and relative computational simplicity, *a priori* pseudopotential calculations in a supercell geometry have increasingly replaced self-consistent Green's function calculations as the most commonly used LDA-based method.

III. HYDROGEN IN SILICON

Not only is hydrogen, the first element in the Periodic Table, a simple place to start in investigating the properties of impurities in semiconductors, it is an impurity with a major technological significance. Hydrogen can passivate both donor and acceptor dopants, as well as lattice defects (see, e. g., References 48-51, and Reference 52 for a review). When added in sufficient concentrations, hydrogen can form a molecular species,[53] and inhibit[54] or contribute to[53] the formation of extended defects. Since hydrogen interacts strongly with so many of the impurities and lattice imperfections that may be found in crystals, the fundamental diffusion behavior of hydrogen in a perfect semiconductor crystal has been difficult to determine experimentally. Both different concentrations of trapping sites for hydrogen, and the space charge fields due to variations in dopant or hydrogen concentration, which may affect the motion of charged hydrogen, have resulted in the wide variety of results reported for hydrogen diffusion at temperatures below 800 K.[55-58]

In order to avoid the complex details of the interactions of hydrogen with various dopants, where much still remains controversial, we will discuss here only the behavior of an isolated hydrogen atom in a perfect silicon crystal. The same basic picture of the total energy for this system as a function of hydrogen position is now supported by calculations using a variety of theoretical techniques.

In order to describe how hydrogen moves through the crystal, the stable and metastable positions where hydrogen prefers to sit must first be identified. In contrast to kinetic behavior, the location of these sites is independent of the mass, and depends only on the chemical nature and bonding properties of hydrogen. Therefore, the stable and metastable positions in the lattice should be the same for hydrogen as for muonium, which may be considered to be a light isotope of hydrogen. There is a substantial amount of experimental data on the characteristics of muonium in semiconductors, which is reviewed in Reference 59. In muon spin rotation experiments, a muonium state with an isotropic hyperfine interaction ("normal" muonium) and a muonium state with a hyperfine interaction that has <111> axial symmetry ("anomalous" muonium) are observed in silicon, diamond, and several other semiconductors with diamond or zincblende lattice structure.

Early theoretical work, including extended Hückel calculations,[60] Green's function calculations,[61] MNDO calculations,[62] and CNDO calculations[63] for hydrogen in silicon, Hartree-Fock calculations for muonium in diamond,[64] and later Hartree-Fock and PRDDO calculations for muonium and hydrogen in diamond[65] and in silicon,[66] considered both high-electron-density sites, on or near the chains of bonded host atoms, and low-electron-density sites, in the open spaces between the bonding chains. These calculations usually included little or no relaxation of the host lattice, and tended to find low-electron-density sites as the energetically favored positions for hydrogen or muonium in the lattice. (Figure 1 shows the position of the low-electron-density tetrahedral and hexagonal sites and the high-electron-density bond-centered site in the lattice. For clarity, not all the positions indicated by various papers as actual minima in the potential energy surface are shown in this figure.) Green's function calculations for a muon assumed to be at the tetrahedral interstitial site in silicon[67] obtained a value very close to the experimental value for the hyperfine coupling constant of normal muonium. While the earliest, simple treatments were later superseded by more exact calculations, and some of the early calculations were later refined, as understanding of how to eliminate surface-defect interactions due to cluster size and surface termination progressed, the conclusion that low-electron-density sites at or near the tetrahedral position were favored energetically for minimal lattice relaxation remained. (See, for example, the later Hartree-Fock and PRDDO calculations for hydrogen and muonium in diamond,[65] which corrected the earlier treatment of bond saturation at the surface,[64] shown in Reference 68 to lead to cluster size dependent results.) More recent calculations[69-70] do not contradict the identification of normal muonium in silicon with a muonium traveling (or tunneling) from one site to another in the low-electron-density channels, where the total energy surface is relatively flat, but trapped in these channels by the lack of time for the large lattice relaxations required to stabilize the muonium at other positions.[70] A similar motion of hydrogen through the low-electron-density channels in silicon has been observed in high temperature molecular dynamics calculations.[71]

The bond-centered position was first suggested as the site for anomalous muonium by Cox and Symons,[72] although Fisch and Licciardello had previously proposed this site as a likely position for hydrogen in amorphous silicon, where a range of silicon-silicon bond lengths, including some of the proper length to accommodate an added hydrogen atom, is expected.[73] According to the three-center-bond model described in Reference 73, the symmetric combination of the sp hybrids on the two silicon neighbors which point toward the hydrogen interacts with the hydrogen s orbital to form a totally symmetric, bonding wave function and an antibonding wave function, while the antisymmetric combination of the silicon hybrids does not interact with the hydrogen s orbital, and remains a non-bonding wave function for the three-center geometry. Since each silicon contributes one electron to fill these electronic states, for positively ionized hydrogen H^+, which has no electron to contribute, only the three-center bonding state should be filled. The three-center geometry should therefore be stable for H^+, if the nearest neighbor silicons are allowed to relax to their preferred distance from the hydrogen. For neutral hydrogen, one electron must go in the non-bonding state, so the three-center-bond configuration is less likely to be stable, and for negatively charged H^-, with the non-bonding state completely filled, this configuration is even less favorable. The identification of the bond-centered site, stabilized by a large relaxation of the neighboring silicon atoms, as the preferred position of muonium or hydrogen in silicon was confirmed initially by the PRDDO calculations,[74-75] and subsequently by MINDO,[76-77] MNDO,[78] and LDA pseudopotential[79-80,69] calculations. The general picture emerging from these calculations is that neutral hydrogen and H^+ prefer to sit at the bond-centered site, while H^- prefers a low-electron-density site. The theoretical identification of the bond-centered site as the position of anomalous muonium[74-75] was also verified subsequently by a muon spin resonance experiment showing the presence of two equivalent silicon nearest neighbors, each bonded to three other silicon atoms,[81] and an experimental observation of a hydrogen center in silicon which has a hyperfine structure similar to that of anomalous muonium, and should therefore also be located at the bond-centered site, was reported.[82-83]

The total energy surface as a function of hydrogen position obtained from LDA pseudopotential calculations[79-80,84] has been used to calculate diffusion coefficients for hydrogen in silicon, assuming the silicon lattice is allowed to relax completely for each hydrogen position.[85] In this work, it is shown that the most energetically favorable path for H^+ (assuming complete lattice relaxation) lets the hydrogen wind its way down the bonding chains between bond-centered sites without ever going out into the low-electron-density channels, while the low and high-electron density paths are similar in energy for neutral hydrogen.[84] However, it is unlikely that the much more massive silicon atoms have time to relax substantially in response to the motion of the hydrogen, as was pointed out, for example, in Reference 86, so that the motion of hydrogen between the bond-centered sites is likely to be determined primarily by the ability of the silicon lattice to assume a position favorable for the new bond-centered location. Molecular dynamics simulations[71] of the high temperature diffusion of H^+ show that the hydrogen most frequently jumps between bond-centered sites by passing through the low-electron-density hexagonal and/or tetrahedral sites, but it can also follow a path lying completely in the low-electron-density region. Due to the large energy barriers which oppose insertion of the hydrogen into a new bond-centered site before the neighboring silicon atoms have had time to relax, tunneling effects (which have not been included in any of the work on hydrogen diffusion through a perfect crystal) are not expected to change the picture substantially, although tunneling of hydrogen around a beryllium atom to which it is bound in a silicon crystal has been both observed[87] and explained theoretically, since in this case an energetically favorable path for the motion which does not involve substantial lattice relaxation has been found.[88]

In summary, although details of the potential energy surface calculated by different theoretical methods may differ and some questions remain, the general picture for hydrogen in a perfect silicon crystal is remarkably clear. One major lesson that has emerged from this work, which was not initially obvious, is that thorough consideration of lattice relaxation is essential, and highly distorted configurations of point defects can turn out to be the most energetically favorable. Unfortunately, no similarly clear conclusions about which of the relevant processes is dominant at high temperature can as yet be drawn from the theoretical work on self-diffusion in silicon.

IV. SILICON SELF-DIFFUSION

The variety of processes and defect configurations which may be important in self-diffusion is larger than for diffusion of hydrogen in a perfect crystal.

Diffusion may occur by motion of vacancies as well as interstitials, or even by direct exchange of atoms on the host lattice, in the absence of point defects. A diffusing self-interstitial may try to share a lattice site with a host atom, in any of several split-interstitial configurations. A large amount of experimental work has been done on diffusion in silicon: for surveys of the more recent work and references to earlier reviews, see References 89 and 90.

Vacancies were the first native point defects in silicon to be extensively studied both theoretically[39-40,91] and experimentally.[92-93] A coherent and reasonably complete picture of the isolated vacancy has resulted. As predicted theoretically,[91,94-95] the vacancy was later experimentally shown[96] to be an Anderson negative-U system:[97] in other words, the singly charged V^+ state was shown to be metastable, decaying either into V^0 or V^{++}, depending on the Fermi energy. The neutral vacancy formation enthalpy[98-101] of about 3.5 eV, and migration enthalpies[102] for the direct path along a bond of 0.3 eV for V^0 and 0.4 eV for V^{++}, calculated by LDA methods, and allowing the lattice to relax completely for each position of the traveling atom, agree well with the experimental values of 3.4eV,[103-104] 0.33 eV, and 0.45 eV,[92-93] respectively. Further LDA calculations show that migration by a distorted path, preserving as many bonds to the traveling atom as possible, seems to be more energetically favorable than vacancy migration by the direct path, along the bond.[105]

Although self-diffusion in silicon appears to be mediated by vacancies at low temperature,[89] the identification of the dominant high temperature diffusion mechanism remains controversial. For an interpretation of the experimental evidence which supports the conclusion that vacancies and not interstitials dominate diffusion at high temperature, see Reference 106. LDA simulations of high temperature vacancy diffusion show strong dynamic effects, which may help explain the large pre-exponential factors seen in high temperature diffusion.[107]

In contrast with vacancies, isolated self-interstitials have never been observed in silicon. Even after radiation at 4.2 K, the displaced self-interstitial appears to migrate rapidly until it displaces a substitutional impurity (or is otherwise trapped), resulting in the observation of impurity interstitials or interstitial-related defect complexes, but no isolated self-interstitials.[108] Early extended Hückel calculations for the carbon interstitial in diamond,[109-110] which were used to suggest similar behavior for the silicon self-interstitial,[112] suggested that athermal migration might be possible, since the predicted minimum-energy configuration changed for different interstitial charge states. These calculations also indicated an apparent preference of the neutral interstitial for a bond-centered or split configuration rather than a low-electron-density tetrahedral or hexagonal interstitial site.

More accurate and elaborate LDA-based calculation were later performed for the tetrahedral and hexagonal configurations of the silicon self-interstitial,[113-115] as well as for several varieties of the split and bond-centered configurations,[98-100,116-117] shown in Figure 1, which were more difficult to treat accurately, due to their lower symmetry and larger lattice relaxations. In all these calculations, the doubly ionized self-interstitial Si^{++} was found to prefer the tetrahedral site, where the electron density is the lowest, while the neutral interstitial was found to prefer sites of higher electron density, such as the hexagonal, bond-centered, and split interstitial sites. Of all the configurations considered in these static calculations, the <110> split configuration, shown in Figure 1 as the X configuration, was found to have the lowest energy for the neutral interstitial.[117] However, the self-interstitial was found to have similar total energies in several configurations. This should result in similar activation enthalpies for several migration paths and large activation entropies. The results also suggest that there may be many paths available for athermal diffusion due to charge carrier capture. LDA-based molecular dynamics calculations in progress have so far confirmed that the neutral X interstitial is stable and that there are large flat regions in the total energy surface as a function of interstitial position, which should give rise to high entropies of formation for silicon self-interstitials.[118]

In summary, both vacancies and interstitials have been found to have formation enthalpies of roughly 4 eV and migration enthalpies of roughly 0.4 eV, giving rise to activation enthalpies for diffusion in the experimental range[89] of 4-5 eV. The large activation enthalpies observed at high temperature, where defects must be created thermally, and the rapid diffusion seen in low temperature radiation experiments, can therefore be explained by the same point defect mechanisms. However, since the calculated activation enthalpies for vacancies and interstitials are similar, it is not possible to resolve the controversy over the dominant mechanism for silicon self-diffusion at high temperature on the basis of presently available theoretical results. To make things still more complicated, the direct exchange mechanism proposed by Pandey, which takes place without point defects, also has an activation enthalpy in the experimental range.[119]

The situation may become somewhat clearer in the near future, with the publication of the results of molecular dynamics simulations of high temperature diffusion mediated by vacancies[107] and interstitials.[118] In the meantime, static LDA-based calculations of the effects of pressure on the activation energies for diffusion by vacancy, interstitial, and concerted exchange mechanisms have suggested that an experimental investigation of diffusion under different pressures be undertaken to determine the dominant mechanism.[120]

V. OTHER SYSTEMS: $Hg_{1-x}Cd_xTe$

Since the same native defects which dominate self-diffusion may also play a role in the diffusion of dopants, work on dopant diffusion in silicon has been closely tied to work on self-diffusion. Because of its intrinsic technological importance as well as its relevance for self-diffusion, there has been much experimental work on dopant diffusion in silicon (surveyed in References 89 and 90, along with some discussion of the points which have remained controversial for dopant diffusion as well as self-diffusion), as well as a number of theoretical calculations. Reference 115, for example, shows that carrier-capture-enhanced diffusion is possible for both aluminum and self-interstitials in silicon. Other LDA-based calculations[101,121] indicate that diffusion for boron, phosphorus, arsenic, and antimony in silicon may proceed down interstitial channels or via a vacancy-assisted process, while the concerted exchange mechanism,[119] which involves no point defects, appears to be less important. Initial LDA-based calculations of the total energy of chalcogen impurities at various sites in silicon, and preliminary applications for diffusion, have been performed.[122-123] Investigation of the rich variety of defect reactions which may be involved in the diffusion of oxygen, carbon, and other impurities in silicon by empirical classical potentials,[124] MNDO,[125] MINDO,[126-7] and other methods has only begun.

Even less is known about impurity and self-diffusion in most other systems. In addition to the early semiempirical work on diffusion in diamond, including the extended Hückel calculations mentioned above, which suggested that the carbon self-interstitial prefers a bond-centered or split configuration rather than a tetrahedral or hexagonal configuration,[109-110] considerably more accurate recent LDA-based calculations have indicated that vacancies rather than interstitials or direct exchange dominate self-diffusion in diamond for all positions of the Fermi level.[128-9] Similar calculations of defect formation energies in SiC show that the antisite defect C_{Si} is favored in C-rich material, while for Si-rich material, the antisite defect Si_C is favored in n-type crystals and the carbon vacancy is favored in p-type crystals.[129-130] Recent calculations of the total energies of various defects in GaAs[131-132] form an initial starting point for an LDA-based investigation of diffusion in this material. Other LDA-based calculations[133] show that a vacancy mechanism appears to be favored for self-diffusion in graphite, although they cannot rule out the possibility of a more complicated direct exchange process than the one considered (as for all static calculations, future consideration of other, more complex diffusion processes, perhaps involving more highly distorted point defect configurations, may show these to be favored over the processes previously considered).

Behavior observed in binary and ternary compounds involves defects which may contain anion or cation atoms, and may be situated at a larger number of distinguishable sites than are found in the diamond lattice of a homopolar crystal. For example, two types of tetrahedral interstitial site occur in the zincblende crystal: sites with cation and with anion nearest neighbors, which we may here call T1 and T2 sites, respectively. The number of available defects and defect complexes in the these systems and the variety of configurations which may be important for diffusion is so great that initial theoretical calculations can only hope to give some additional direction for further experimental and theoretical work.

The current state of understanding of Cd and Hg diffusion in CdTe and $Hg_{1-x}Cd_xTe$ alloys may be considered to be illustrative of the situation for many of the III-V and II-VI semiconductors, where a reproducible experimental characterization of the diffusion does not always bring with it a coherent understanding of the microscopic process, or even which point defects are responsible for the diffusion, and how they contribute to observed electrical behavior and other properties of the material. Recent tracer diffusion results[135-140] on self-diffusion of Cd, Hg, and Te in $Hg_{0.8}Cd_{0.2}Te$ have produced a reasonably reproducible experimental characterization, despite considerable inconsistency in the early experimental work (reviewed in References 134 and 135). Mercury profiles, which are unchanged by preannealing, may be fitted by a sum of two complementary error function (ERFC) curves. The slower component appears to be independent of the mercury partial pressure, p_{Hg}, while the diffusion coefficient of the fast component is proportional to p_{Hg} at high mercury pressures and to p_{Hg}^{-1} at low mercury pressures.[135-138] (Brown and Willoughby[134,141] see additional, faster components after diffusion anneals at 225°C, instead of the slow component seen in References 135-138 and 140, which may have been too slow to observe at their diffusion temperature and annealing time.) Two components are also seen for Cd diffusion (except for Reference 139, which reports only one component). At 350°C and above, Cd diffusion appears to be independent of the mercury partial pressure (which determines the partial pressures of the other components as well[142]), except for an increase near the maximum value of p_{Hg}.[135-139]

The behavior of Cd in $Hg_{0.8}Cd_{0.2}Te$ is similar to Cd self-diffusion behavior observed in CdTe (reviewed in Reference 144). Aside from the small increase in Cd diffusion observed for CdTe under higher Cd pressures (corresponding to the similar increase observed in $Hg_{0.8}Cd_{0.2}Te$), which has been attributed to the increasing importance of Cd interstitials, the dominant mechanisms suggested for Cd diffusion in CdTe include a pressure-independent exchange process which does not involve point defects, or a process involving a neutral defect complex, perhaps consisting of a Cd vacancy and a Cd interstitial.[144-145] Shaw[139] suggests that complexes of native defects could account for Cd diffusion in $Hg_{0.8}Cd_{0.2}Te$. Tang and Stevenson[135] suggest that a complex mechanism involving both a Cd interstitial and a cation vacancy is responsible for the pressure independence of Cd diffusion, while vacancy and interstitial mechanisms operating in parallel are responsible for the pressure dependence observed for the fast component of Hg diffusion in $Hg_{0.8}Cd_{0.2}Te$. However, the Tang and Stevenson model of vacancy-interstitial diffusion in series[135] for Cd diffusion does not explain why the interstitial step must be followed immediately by the vacancy step, instead of occurring repeatedly as a purely interstitial kick-out diffusion process, in parallel with any existing vacancy-mediated processes. Tang and Stevenson's belief[135] that the fast component seen for mercury represents true self-diffusion in the bulk, rather than some sort of short-circuit or pipe diffusion, has also been questioned.[140]

The earliest assistance for experimental interpretation and planning in HgCdTe was obtained from semiempirical estimates of bond energies and point defect formation energies. These estimates have now been followed by tight-binding calculations of the total energies of isolated vacancies[25,147] and interstitials in various configurations,[23-25,146] and subsequently linear muffin-tin orbital calculations using the atomic spheres approximation (LMTO-ASA)[148] for interstitials in the two tetrahedral positions and antisite defects. Lattice relaxation was included in some of the interstitial calculations (References 23-25); however, a complete investigation including highly distorted interstitial configurations has not yet been done, and no defect complexes have yet been considered.

Specific conclusions which may be drawn from this work include the suggestion that Te antisite defects may be more important than previously assumed: these defects appear to have a favorable total energy,[148] and the creation of these defects may be promoted in Te-rich material by a strain-mediated interaction between Te interstitials and cation vacancies.[25] The attraction of interstitials, which have an outward nearest-neighbor relaxation, to vacancies, which have an inward nearest-neighbor relaxation, should be particularly strong for Te, since the calculated relaxation for the preferred tetrahedral interstitial position was larger for Te than for all the other native or dopant interstitials considered.[25] The large strain energy associated with Te interstitials may also help to explain the tendency for excess Te to condense into second phase inclusions.[25]

Interstitial diffusion down the open channels between tetrahedral sites, passing through the hexagonal sites, was initially considered[146] by comparing total energies at the two tetrahedral sites, as the original tight-binding treatment did not permit a reliable direct comparison of total energies at interstitial sites with different coordination.[6-8,26-28] Estimated diffusion barriers obtained in this way indicated that direct interstitial diffusion down the open channels appeared to be energetically favorable for Hg, but unfavorable for Cd, which must therefore diffuse by some more complicated mechanism.[146] Subsequent calculations showing that large strains (and strain energies) are associated with Cd interstitials at T1 and hexagonal sites[25] may help explain the apparent unfavorability[146,135] of Cd interstitial diffusion down the open channels between preferred tetrahedral (T2) sites. For Hg diffusion, where a simple interstitial mechanism appears to be energetically favorable,[146,135] the possibility that diffusion could be enhanced by charge carrier capture was suggested,[146] since the preferred charge state changes with position,[149-150] going from neutral in the T1 position to doubly charged Hg^{++} in the preferred tetrahedral (T2) and hexagonal positions.

Obviously much more work, both theoretical and experimental, will need to be done before the atomic processes which occur during Hg and Cd diffusion in CdTe and $Hg_{1-x}Cd_xTe$ are fully understood. All this work will be complicated by the interactions of native point defects with impurities, and with any strains which may be present in the lattice as a result of nearby extended defects, surfaces, or interfaces. For example, a strong dependence of point defect formation energies on these strains in the lattice could result in strongly inhomogeneous point defect concentrations and diffusion constants, perhaps producing effects such as the depth-dependent diffusion recently observed in HgCdTe superlattices.[151-152]

VI. CONCLUSIONS

The characteristics, advantages, and shortcomings of the basic theoretical methods used to investigate point defects and diffusion in semiconductors have been briefly reviewed. While these methods differ widely in accuracy and computational expense, all use approximations which cause errors in point defect total energies and diffusion barriers that cannot be precisely estimated, except by appeal to test calculations on similar systems. Both the development of tight-binding calculations based on first-principles Hamiltonians, for the initial exploration of systems where many defects or many configurations must be considered, and corrections leading to an improved band gap for the more accurate and expensive LDA-based defect calculations, should lead to expanded theoretical capabilities in the foreseeable future.

The history and current status of theoretical work on hydrogen diffusion in silicon, silicon self-diffusion, and diffusion of Hg and Cd in HgCdTe have also been described, as examples of a system where a basically coherent picture has been achieved, a system where the many theoretical contributions have still not resolved a fundamental controversy, and a system where only the very first steps have been taken toward a theoretical understanding of diffusion. Aside from the specifics of what has been learned for each system, the theoretical calculations on hydrogen and self-interstitials in silicon have contributed to the growing realization of the importance of point defect configurations involving considerable relaxation of neighboring atoms. The realization that the preferred configuration of a defect is not always the most obvious one has made the value of the new molecular dynamics methods, which allow the defect and the surrounding lattice to relax freely and simultaneously, very apparent. This, together with the new understanding of dynamic effects, unexplained by static total energy calculations, which is being reached by molecular dynamics calculations for hydrogen and self-diffusion in silicon, makes the advent of these methods the third exciting new development, from which much can be expected in the future.

ACKNOWLEDGMENTS

This work was supported by the Night Vision and Electro-Optics Laboratories and the ARO under ARO Grant No. DAAL03-87-K-0061, and by the Institute for Manufacturing Research.

REFERENCES

[1] W. Kohn and L. J. Sham, Phys. Rev. 140, A1133 (1965).

[2] L. J. Sham and W. Kohn, Phys. Rev. 145, 561 (1966).

[3] *Theory of the Inhomogeneous Electron Gas*, edited by N. H. March and S. Lundqvist (Plenum, New York, 1983).

[4] R. Car and M. Parrinello, Phys. Rev. Lett. 55, 2471 (1985).

[5] A. P. Sutton, M. W. Finnis, D. G. Pettifor, and Y. Ohta, J. Phys. C 21, 35 (1988).

[6] D. J. Chadi, in *Atomistic Simulation of Materials: Beyond Pair Potentials*, edited by V. Vitek and D. J. Srolovitz (Plenum, New York, 1989) and references therein.

[7] W. M. C. Foulkes and R. Haydock, Phys. Rev. B 39, 12520 (1989), and references therein.

[8] O. F. Sankey and D. J. Niklewski, Phys. Rev. B 40, 3979 (1989), and references therein.

[9] The LDA-based methods tend to give band gaps that are too small, which leads to inaccuracies in electronic levels derived from the conduction band for systems containing defects, and incorrect total energies for defect systems when these defect levels are occupied. Much work, including the following references (10-16), has been done on correcting the LDA-based methods for bulk calculations, but not yet for systems involving defects.

[10] G. Strinati, H. J. Mattausch, and W. Hanke, Phys. Rev. B 25, 2867 (1982).

[11] J. P. Perdew and M. Levy, Phys. Rev. Lett. 51, 1884 (1983).

[12] L. J. Sham and M. Schlüter, Phys. Rev. Lett. 51, 1888 (1983), and Phys. Rev. B 32, 3883 (1985).

[13] W. E. Pickett and C. S. Wang, Phys. Rev. B 30, 4719 (1984).

[14] M. Lannoo, M. Schlüter, and L. J. Sham, Phys. Rev. B 32, 3890 (1985).

[15] M. Hybertson and S. G. Louie, Phys. Rev. Lett. 55, 1418 (1985), and Phys. Rev. B 34, 5390 (1986).

[16] R. W. Godby, M. Schlüter, and L. J. Sham, Phys. Rev. Lett. 56, 2415 (1986), and Phys. Rev. B 35, 4170 (1987).

[17] For (110) surfaces of Group IV, III-V, and II-VI semiconductors: D. J. Chadi, Phys. Rev. Lett. 41, 1062 (1978), and Phys. Rev. B 19, 2074 (1979).

[18] For silicon (211), (311), and (331) surfaces: D. J. Chadi, Phys. Rev. B 29, 785 (1984).

[19] For silicon (111) 7x7 surface structure: G. X. Qian and D. J. Chadi, Phys. Rev. B 35, 1288 (1987).

[20] For GaAs (100) surface: D. J. Chadi, J. Vac. Sci. Technol. A 5, 834 (1987).

[21] For silicon (100) and stepped (100) surfaces: D. J. Chadi, J. Vac. Sci. Technol. 16, 1290 (1979), Phys. Rev. Lett. 43, 43 (1979), and

Phys. Rev. Lett. 59, 1691 (1987).

[22] Relaxation predicted in Reference 21 verified experimentally, e. g. by P. E. Wierenga, J. A. Kubby, and J. E. Griffith, Phys. Rev. Lett. 59, 2169 (1987).

[23] J. T. Schick and C. G. Morgan-Pond, Bull. Am. Phys. Soc. 34, 456 (1989), and to be published.

[24] J. T. Schick and C. G. Morgan-Pond, Semicond. Sci. Technol. 5, S81 (1990).

[25] J. T. Schick and C. G. Morgan-Pond, J. Vac. Sci. Technol. A 8, 1108 (1990).

[26] D. Tománek and M. A. Schlüter, Phys. Rev. Lett. 56, 1055 (1986).

[27] D. Tománek and M. A. Schlüter, Phys. Rev. B 36, 1208 (1987).

[28] D. Tománek, C. Sun, N. Sharma, and L. Wang, Phys. Rev. B 39, 5361 (1989).

[29] O. K. Andersen and O. Jepsen, Phys. Rev. Lett. 53, 2571 (1984).

[30] T. A. Halgren and W. N. Lipscomb, J. Chem. Phys. 58, 1569 (1973).

[31] D. S. Marynick and W. N. Lipscomb, Proc. Nat. Acad. Sci. (USA) 79, 1341 (1982).

[32] See, e. g., S. Estreicher, A. K. Ray, J. L. Fry, and D. S. Marynick, Phys Rev. B 34, 6071 (1986).

[33] J. A. Pople and D. L. Beveridge, *Approximate Molecular Orbital Theory* (McGraw-Hill, New York, 1970).

[34] M. J. S. Dewar and W. Thiel, J. Am. Chem. Soc. 99, 4899 (1977), and J. Am. Chem. Soc. 99, 4907 (1977).

[35] M. J. S. Dewar, M. L. McKee, and H. S. Rzepa, J. Am. Chem. Soc. 100, 3607 (1978).

[36] R. C. Bingham, M. J. S. Dewar, and D. C. Lo, J. Am. Chem. Soc. 97, 1285 (1975).

[37] K. H. Johnson and F. C. Smith, Phys. Rev. B 5, 831 (1972).

[38] K. Schwarz, Phys. Rev. B 5, 2466 (1972).

[39] G. A. Baraff and M. Schlüter, Phys. Rev. B 19, 4965 (1979).

[40] J. Bernholc, N. O. Lipari, and S. T. Pantelides, Phys. Rev. B 21, 3545 (1980).

[41] Basic theory reviewed by M. L. Cohen and V. Heine in *Solid State Physics*, Vol. 24, edited by H. E. Ehrenreich, F. Seitz, and D. Turnbull (Academic Press, New York, 1970), p. 38.

[42] D. R. Hamann, M. Schlüter, and C. Chiang, Phys. Rev. Lett. 43, 1494 (1979).

[43] G. B. Bachelet, D. R. Hamann, and M. Schlüter, Phys. Rev. B 26, 4199 (1982).

[44] M. Lannoo, in *Proceedings of the 19th International Conference on the Physics of Semiconductors*, Vol. 2, edited by W. Zawadzki (Institute of Physics, Polish Academy of Sciences, Wroclaw, Poland, 1988), p. 951.

[45] F. Beeler, M. Scheffler, O. Jepsen, and O. Gunnarsson, Phys. Rev.

Lett. 54, 2525 (1985).

[46] R. Car, P. J. Kelly, A. Oshiyama, and S. T. Pantelides, Phys. Rev. Lett. 52, 1814 (1984).

[47] See, e. g., S. Estreicher, Phys. Rev. B 37, 858 (1988).

[48] N. M. Johnson, C. Herring, and D. J. Chadi, Phys. Rev. Lett. 56, 769 (1986).

[49] J. I. Pankove, D. E. Carlson, J. E. Berkeyheiser, and R. O. Wance, Phys. Rev. Lett. 51, 2224 (1983).

[50] J. I. Pankove, R. O. Wance, and J. E. Berkeyheiser, Appl. Phys. Lett. 45, 1100 (1984).

[51] J. I. Pankove, P. J. Zancucchi, and C. W. Magee, Appl. Phys. Lett. 46, 421 (1985).

[52] S. J. Pearton, J. W. Corbett, and T. S. Shi, Appl. Phys. A 43, 153 (1987).

[53] N. M. Johnson and C. Herring, in *Proceedings of the 19th International Conference on the Physics of Semiconductors*, Vol. 2, edited by W. Zawadzki (Wroclaw, Poland, Institute of Physics, Polish Academy of Sciences, 1988), p. 1137.

[54] A. J. R. DeKock, S. D. Ferris, L. C. Kimerling, and H. J. Leamy, Appl. Phys. Lett. 27, 313 (1975).

[55] T. Ichimiya and A. Furuichi, Int. J. Appl. Radiat. Isot. 19, 573 (1968).

[56] S. J. Pearton, J. Electron. Mater. 14a, 737 (1985).

[57] C. H. Seager, R. A. Anderson, and J. K. G. Panitz, J. Mater. Res. 2, 96 (1987).

[58] C. H. Seager and R. A. Anderson, Appl. Phys. Lett. 53, 1181 (1988).

[59] B. D. Patterson, Rev. Mod. Phys. 60, 69 (1988).

[60] V. A. Singh, C. Weigel, J. W. Corbett, and L. M. Roth, Phys. Stat. Sol. (b) 81, 637 (1977).

[61] C. O. Rodriguez, M. Jaros, and S. Brand, Solid State Commun. 31, 43 (1979).

[62] J. W. Corbett, S. N. Sahu, T. S. Shi, and L. C. Snyder, Phys. Lett. 93A, 303 (1983).

[63] A. Mainwood and A. M. Stoneham, J. Phys. C 17, 2513 (1984).

[64] N. Sahoo, S. K. Mishra, K. C. Mishra, A. Coker, T. P. Das, C. K. Mitra, L. C. Snyder, and A. Glodeanu, Phys. Rev. Lett. 50, 913 (1983).

[65] S. Estreicher, A. K. Ray, J. L. Fry, and D. S. Marynick, Phys. Rev. B 34, 6071 (1986).

[66] N. Sahoo, K. C. Mishra, and T. P. Das, Hyperfine Interact. 32, 601 (1986).

[67] H. Katayama-Yoshida and K. Shindo, Phys. Rev. Lett. 51, 207 (1983).

[68] S. Estreicher, A. K. Ray, J. L. Fry, and D. S. Marynick, Phys. Rev. Lett. 55, 1976 (1985).

[69] C. G. Van de Walle, in *Hydrogen in Semiconductors*, edited by J. I.

Pankove and N. M. Johnson (Academic Press, New York, 1990), in press.

[70] C. H. Chu and S. K. Estreicher, to be published.

[71] F. Buda, G. L. Chiarotti, R. Car, and M. Parrinello, Phys. Rev. Lett. 63, 294 (1989).

[72] S. F. J. Cox and M. C. R. Symons, Chem. Phys. Lett. 126, 516 (1986).

[73] R. Fisch and D. C. Licciardello, Phys. Rev. Lett. 41, 889 (1978).

[74] T. L. Estle, S. Estreicher, and D. S. Marynick, Hyperfine Interact. 32, 637 (1986).

[75] S. Estreicher, Phys. Rev. B 36, 9122 (1987).

[76] P. Deak, L. C. Snyder, and J. W. Corbett, Phys. Rev. B 37, 6887 (1988).

[77] P. Deak, L. C. Snyder, J. L. Lindstrom, J. W. Corbett, S. J. Pearton, and A. J. Tavendale, Phys. Lett. A 126, 427 (1988).

[78] G. G. DeLeo, M. J. Dorogi, and W. B. Fowler, Phys. Rev. B 38, 7520 (1988).

[79] C. G. Van de Walle, Y. Bar-Yam, and S. T. Pantelides, Phys. Rev. Lett. 60, 2761 (1988).

[80] C. G. Van de Walle, P. J. H. Denteneer, Y. Bar-Yam, and S. T. Pantelides, Phys. Rev. B 39, 10791 (1989).

[81] R. F. Kiefl, M. Celio T. L. Estle, S. R. Kreitzman, G. M. Luke, T. M. Riseman, and E. J. Ansaldo, Phys. Rev. Lett. 60, 224 (1988).

[82] Yu. V. Gorelkinskii and N. N. Nevinnyi, Pisma Zh. Tekh. Fiz. 13, 105 (1987).

[83] R. B. Gel'fand, V. A. Gordeev, Yu. V. Gorelkinskii, R. F. Konopleva, S. A. Kuten', A. V. Mudryi, N. N. Nevinnyi, Yu. V. Obukhov, V. I. Rapoport, A. G. Ul'yashin and V. G. Firsov, Sov. Phys. Solid State 31, 1376 (1989).

[84] P. J. H. Denteneer, C. S. Nichols, C. G. Van de Walle, and S. T. Pantelides, in *Proceedings of the 19th International Conference on the Physics of Semiconductors*, Vol. 2, edited by W. Zawadzki (Institute of Physics, Polish Academy of Sciences, Wroclaw, Poland, 1988), p. 999.

[85] P. E. Blöchl, C. G. Van de Walle, and S. T. Pantelides, Phys. Rev. Lett. 64, 1401, (1990).

[86] G. D. Watkins, Mat. Sci. Forum 38-41, 39 (1989).

[87] K. Muro and A. J. Sievers, Phys. Rev. Lett. 57, 897 (1986).

[88] P. J. H. Denteneer, C. G. Van de Walle, and S. T. Pantelides, Phys. Rev. Lett. 62, 1884 (1989).

[89] W. Frank, U. Gösele, H. Mehrer, and A. Seeger, in *Diffusion in Crystalline Solids*, edited by G. E. Murch and A. S. Nowick (Academic Press, Orlando, 1984), p. 63.

[90] P. M. Fahey, P. B. Griffin, and J. D. Plummer, Rev. Mod. Phys 61, 289 (1989).

[91] G. A. Baraff, E. O. Kane, and M. Schlüter, Phys. Rev. B 21, 5662 (1980), and references therein.

[92] G. D. Watkins, J. Phys. Soc. Japan 18, Suppl. II, 22 (1963).

[93] G. D. Watkins, in *Deep Centers in Semiconductors*, edited by S. T. Pantelides, (Gordon and Breach, New York, 1986), p. 147, and references therein.

[94] G. A. Baraff, E. O. Kane, and M. Schlüter, Phys. Rev. Lett. 43, 956 (1979).

[95] G. A. Baraff, E. O. Kane, and M. Schlüter, Phys. Rev. B 21, 3563 (1980).

[96] G. D. Watkins and J. R. Troxell, Phys. Rev. Lett. 44, 593 (1980).

[97] P. W. Anderson, Phys. Rev. Lett. 34, 953 (1975).

[98] R. Car, P. J. Kelly, A. Oshiyama, and S. T. Pantelides, J. Electron. Mat., 14a, 269 (1985).

[99] See footnote 6 in R. Car, P. J. Kelly, A. Oshiyama, and S. T. Pantelides, Phys. Rev. Lett. 54, 360 (1985).

[100] Y. Bar-Yam and J. D. Joannopoulos, J. Electron. Mat., 14a, 261 (1985).

[101] C. S. Nichols, C. G. Van de Walle, and S. T. Pantelides, Phys. Rev. B 40, 5484 (1989).

[102] P. J. Kelly, R. Car, and S. T. Pantelides, Mat. Sci. Forum 10-12, 115 (1986).

[103] S. Dannefaer, P. Mascher, and D. Kerr, Phys. Rev. Lett. 56, 2195 (1986).

[104] S. Dannefaer, Mat. Sci. Forum 10-12, 103 (1986).

[105] Y. Bar-Yam and J. D. Joannopoulos, in *Proceedings of the 17th International Conference on the Physics of Semiconductors*, edited by J. D. Chadi and W. A. Harrison (Springer-Verlag, New York, 1985), p. 721.

[106] J. A. Van Vechten, U. Schmid, and N. C. Myers, in *Proceedings of the International Conference on the Science and Technology of Defect Control in Semiconductors*, edited by K. Sumino (North-Holland, Amsterdam, 1989).

[107] E. Smargiassi and R. Car, Bull. Am. Phys. Soc. 35, 621 (1990), and to be published.

[108] G. D. Watkins, in *Radiation Damage in Semiconductors*, edited by P. Baruch (Dunod, Paris, 1965), p. 97.

[109] G. D. Watkins, R. P. Messmer, C. Weigel, D. Peak, and J. W. Corbett, Phys. Rev. Lett. 27, 1573 (1971).

[109] C. Weigel, D. Peak, J. W. Corbett, G. D. Watkins, and R. P. Messmer, Phys. Rev. B 8, 2906 (1973).

[110] C. Weigel and J. W. Corbett, Z. Physik B 23, 233 (1976).

[112] J. W. Corbett, R. L Kleinhenz, E. Wu, and Z. You, J. Nucl. Mat. 108-109, 617 (1982).

[113] Y. Bar-Yam and J. D. Joannopoulos, Phys. Rev. Lett. 52, 1129 (1984).

[114] Y. Bar-Yam and J. D. Joannopoulos, Phys. Rev. B 30, 1844 (1984).

[115] G. A. Baraff and M. Schlüter, Phys. Rev. B 30, 3460 (1984).

[116] R. Car, P. J. Kelly, A. Oshiyama, and S. T. Pantelides, Phys. Rev. Lett. 52, 1814 (1984).

[117] Y. Bar-Yam and J. D. Joannopoulos, Phys. Rev. B 30, 2216 (1984).

[118] P. Blöchl, private communication.

[119] K. C. Pandey, Phys. Rev. Lett. 57, 2287 (1986).

[120] A. Antonelli and J. Bernholc, Phys. Rev. B 40, 10643 (1989).

[121] C. S. Nichols, C. G. Van de Walle, and S. T. Pantelides, Phys. Rev. Lett. 62, 1049 (1989).

[122] F. Beeler, M. Scheffler, O. Jepsen, and O. Gunnarsson, Phys. Rev. Lett. 54, 2525 (1985).

[123] F. Beeler and M. Scheffler, in *Proceedings of the 19th International Conference on the Physics of Semiconductors*, Vol. 2, edited by W. Zawadzki (Institute of Physics, Polish Academy of Sciences, Wroclaw, Poland, 1988), p. 983.

[124] J. Tersoff, Phys. Rev. Lett. 64, 1757 (1990).

[125] G. G. DeLeo, C. S. Milsted, and J. C. Kralik, Phys. Rev. B 31, 3588 (1985).

[126] L. C. Snyder, J. W. Corbett, P. Deak, and R. Wu, Mat. Res. Soc. Symp. Proc. 104, 179 (1988).

[127] P. Deak, L. C. Snyder, J. W. Corbett, R. Z. Wu, and A. Solyom, Mat. Sci. Forum 38-41, 281 (1989).

[128] J. Bernholc, A. Antonelli, T. M. Del Sole, Y. Bar-Yam, and S. T. Pantelides, Phys. Rev. Lett. 61, 2689 (1988).

[129] J. Bernholc, A. Antonelli, C. Wang, and R. F. Davis, in *Proceedings of the 19th International Conference on the Physics of Semiconductors*, Vol. 2, edited by W. Zawadzki (Institute of Physics, Polish Academy of Sciences, Wroclaw, Poland, 1988), p. 1115.

[130] C. Wang, J. Bernholc, and R. F. Davis, Phys. Rev. B 38, 12752 (1988).

[131] G. A. Baraff and M. Schlüter, Phys. Rev. Lett. 55, 1327 (1985).

[132] G. A. Baraff and M. Schlüter, Phys. Rev. Lett. 55, 2340 (1985).

[133] E. Kaxiras and K. C. Pandey, Phys. Rev. Lett. 61, 2693, (1988).

[134] M. Brown and A. F. W. Willoughby, J. Cryst. Growth 59, 27 (1982).

[135] M.-F. S. Tang and D. A. Stevenson, J. Vac. Sci. Technol. A 7, 544 (1989).

[136] M.-F. Sung Tang and D. A. Stevenson, J. Vac. Sci. Technol. A 6, 2650 (1988).

[137] J. S. Chen, F. A. Kröger, and W. L. Ahlgren, Extended Abstracts of the 1984 U. S. Workshop on the Physics and Chemistry of Mercury Cadmium Telluride, p. 109 (unpublished).

[138] J. S. Chen, Ph. D. thesis, University of Southern California, 1985.

[139] D. Shaw, Phil. Mag. A 53, 727 (1986).

[140] N. Archer and H. Palfrey, to be published.

[141] M. Brown and A. F. W. Willoughby, J. Vac. Sci. Technol. A 1, 1641

(1983).

142 R. F. Brebrick, J. Phys. Chem. Solids 40, 177 (1979).

143 T. Tung, L. Golonka, and R. F. Brebrick, J. Electrochem. 128, 451 (1981).

144 K. Zanio, *Cadmium Telluride*, edited by R. K. Willardson and A. C. Beer (Academic Press, New York, 1978).

145 S. S. Chern and F. A. Kröger, J. Solid State Chem. 14, 44 (1975).

146 C. G. Morgan-Pond, J. T. Schick, and S. Goettig, J. Vac. Sci. Technol. A 7, 354 (1989).

147 M. A. Berding, A. Sher, A.-B. Chen, and R. Patrick, Semicond. Sci. Technol. 5, S86 (1990).

148 M. A. Berding, M. van Schilfgaarde, A. T. Paxton, and A. Sher, J. Vac. Sci. Technol. A 8, 1103 (1990).

149 S. Goettig and C. G. Morgan-Pond, J. Vac. Sci. Technol. A 6, 2670 (1988).

150 S. Goettig and C. G. Morgan-Pond, Phys. Rev. B, to be published.

151 Y. Kim, A. Ourmazd, and R. D. Feldman, J. Vac. Sci Technol.A 8, 1116 (1990).

151 Y. Kim, A. Ourmazd, M. Bode, and R. D. Feldman, Phys. Rev. Lett. 63, 636 (1989).

FIGURE CAPTION

Fig. 1. The tetrahedral (T), hexagonal (H), and bond-centered (B) interstitial positions in the diamond or zincblende lattice. Two types of split interstitial are shown, with the two atoms which share one atomic site in the host lattice relaxed along the <110> (X) and <001> (S) directions.

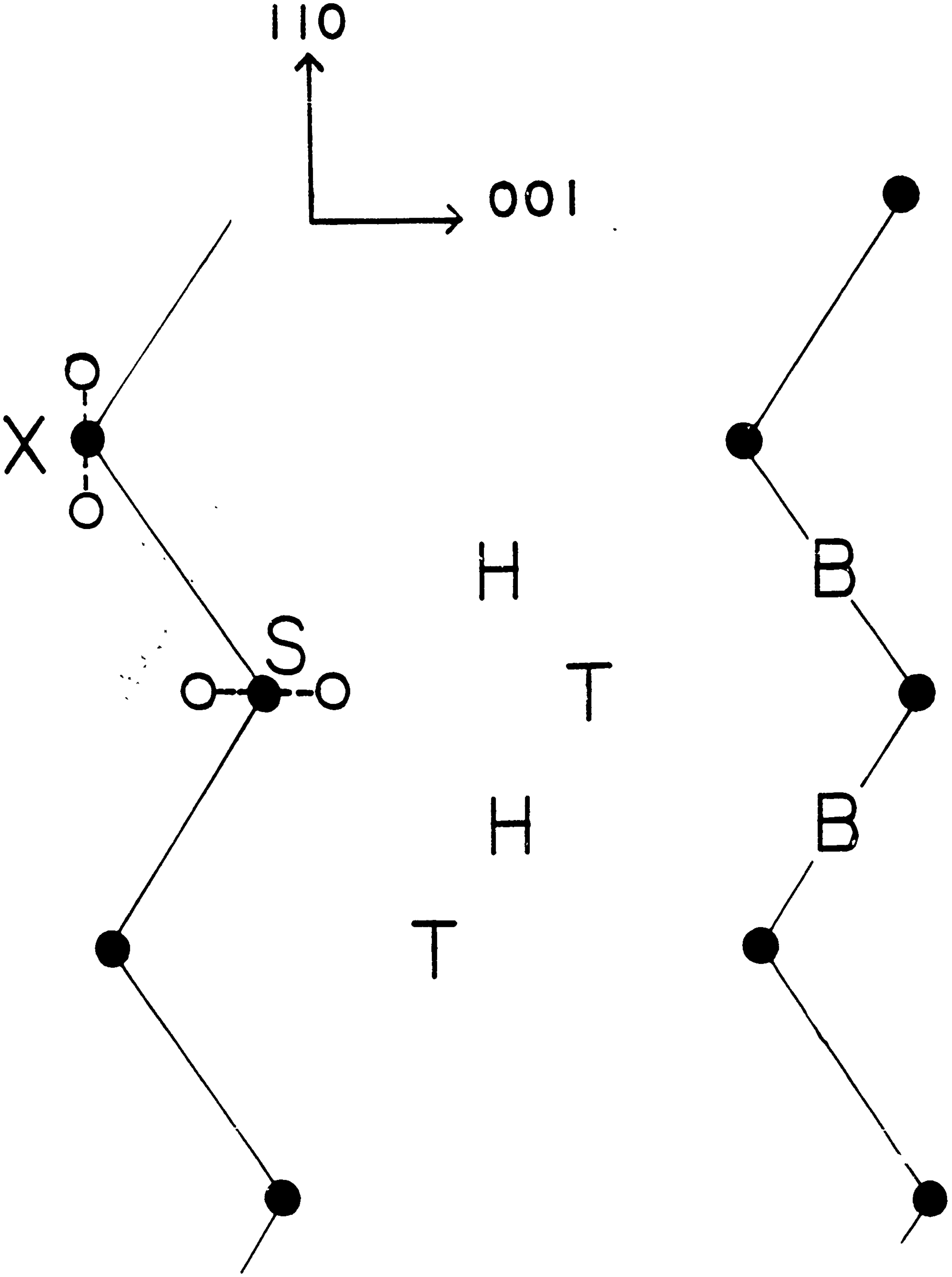
110
001
X
S
H
T
H
T
B
B

Figure 1.